

**An Experimental Investigation of the Effect of Heater Surface  
Preparation Method on Pool Boiling of Nanofluids**

**An Experimental Investigation of the Effect of Heater Surface  
Preparation Method on Pool Boiling of Nanofluids**

**By**

**Naief Almalki, B. Sc.**

**A Thesis**

**Submitted to the School of Graduate Studies**

**in Partial Fulfilment of the Requirements**

**for the Degree**

**Master of Applied Sciences**

**McMaster University**

**Hamilton, Ontario, Canada**

© Copyright by Naief Almalki, August 2015

MASTERS OF APPLIED SCIENCES (2015) (Mechanical Engineering)	McMaster University  Hamilton, Ontario, Canada
TITLE:	An Experimental Investigation of the Effect of Heater Surface Preparation Method on Pool Boiling of Nanofluids
AUTHOR:	Naief Almalki, B. Sc. (Umm Al- Qura University)
SUPERVISOR:	Dr. Mohamed Hamed
NUMBER OF PAGES:	74

## Abstract

An experimental investigation was carried out to study the effect of heater surface preparation on pool boiling of nanofluids. The boiling surface was prepared using different methods: (1) using a diamond turning machine, (2) a conventional lathe machine, and (3) polished using emery sandpaper. The average surface roughness of the diamond turning machined surface was 6 nm and 470 nm for the surfaces prepared using the lathe and sandpaper. The boiling surfaces considered in this study are flat copper surfaces with a diameter of 25.4 mm.  $\text{Al}_2\text{O}_3$ -Water nanofluids prepared using nanoparticles with an initial size of 10 nm and concentration of 0.05%wt were used throughout the present study. In order to improve the nanofluids stability Sodium dodecylbenzenesulfonate (SDBS) was added to the base fluid (water) with a concentration of 0.1%wt. In order to understand the effect of the nanofluids and the surfactant separately and together, pool boiling experiments using distilled water only, nanofluids, distilled water plus the SDBS surfactant, and nanofluids mixed with SDBS (nanosuspensions) were carried out on clean surfaces. The nanofluids and nanosuspensions boiling experiments were followed by distilled water boiling experiments in order to assess the change of the surface characteristics due to any nanoparticles deposition. The same set of boiling experiments was carried out on each of the three prepared surfaces.

The experimental results indicated that for the smooth and rough machined surfaces, the heat transfer coefficient was increased for the nanofluids and the nanosuspensions with respect to distilled water. Distilled water boiling experiments on the unclean (used) surfaces showed that the heat transfer behavior is almost similar to the distilled water on the clean surface, which indicates that the deposition on the smooth

and rough machined surfaces was minimal and hence the enhancement in the heat transfer was due to the change in the thermo-physical properties of the nanofluids and not due to the change in the heater surface condition.

A similar trend was observed in the case of the polished surface in which case nanofluids and nanosuspensions resulted in an enhancement in the rate of heat transfer. However, distilled water boiled on unclean surfaces showed that the boiling curve has shifted to the left compared with the curve of the distilled water on the clean surface. Boiling of distilled water on unclean surfaces showed that the boiling curve was enhanced, which can be attributed to the change in the surface condition and the change in the thermo-physical properties of nanofluids. Photographs of the boiling surfaces and surface measurements taken before and after the nanofluids and nanosuspensions experiments showed that the machined surfaces had less nanoparticles deposition than the sandpaper polished surface. These results indicate that the method of surface preparation has a significant effect on nanoparticles deposition and consequently on the pool boiling heat transfer in which the polished surface tends to have higher number of the active nucleation sites.

## **Acknowledgement**

All praises and thanks are due to Allah (God) first and foremost .

I would like to thank my supervisor Dr. Hamed for his guidance and encouragement during this research .

I also want to give special thanks to lap mate and one of my best friend Mohamed Hamda, you made this research a memorable by your great discussion and encouragement.

Finally, I would like to give my sincere thanks to my family , my mom ,my wife and my little princess Sadeem , I really will not forget what you did for me.

## Table of Contents

Chapter 1 Introduction .....	1
1.1 Pool Boiling .....	1
1.1.1 Natural Convection .....	1
1.1.2 Nucleate Boiling .....	2
1.1.3 Transition Boiling .....	3
1.1.4 Film Boiling .....	3
1.2 Nanofluids.....	3
Chapter 2 Literature Review and Research Objectives and Plan.....	5
2.1 Effect of Surface Condition on Boiling Heat Transfer of Pure Liquids.....	5
2.2 Investigations carried out on Pool Boiling of Nanofluids.....	8
2.4 Effect of Nanoparticles Deposition on the Boiling Surface.....	14
2.5 Summary and Objectives of the Present Study .....	15
2.7 Thesis Structure .....	17
Chapter 3 Experiments Setup and Methodology .....	18
3.1 Experimental Setup.....	18
3.1.1 Heaters Control .....	21
3.1.2 Data Acquisition .....	22
3.2 Thermocouple Calibration .....	22
3.3 Surface Roughness Measurements.....	23
3.4 Surface Preparation.....	24
3.4.1 The Ultra Smooth Surface, Prepared Using a Diamond Turning Machine.....	24
3.4.2 Rough Surface 1, Prepared using a Conventional Lathe Machine.....	25
3.4.3 Rough Surface 2 prepared using Emery Sandpaper.....	27
Figure 3.7 The profile of the boiling surface produced by emery sandpaper with average surface roughness of 470 nm.....	27
3.5 High Speed Imaging of the Boiling Process: .....	28
3.7 Uncertainty Analysis.....	31
3.7.1 Uncertainty in Calculating the Surface Temperature ( $T_s$ ).....	32
3.7.2 Uncertainty in the Calculation of the Surface Heat Flux ( $q''$ ).....	32

3.7.3 Uncertainty in Bulk Fluid Liquid Saturation Temperature $T_{sat}$ .....	32
3.7.4 Uncertainty in the Calculated Surface Superheat ( $T_s - T_{sat}$ ) .....	33
3.8 Nanofluids Preparation .....	34
3.9 Experiment Procedures .....	36
3.10 Parameters Investigated and Experimental Conditions.....	37
Chapter 4 Results and Discussion.....	40
4.1 Validation of the Experimental Setup.....	40
4.2 Repeatability Test .....	41
4.3 Effect of the Boiling Fluid on the Rate of Boiling Heat Transfer.....	43
4.3.1 Results Obtained using Surface 1(Ra=6 nm) .....	43
4.3.2 Results Obtained using Surface 2 (Ra=470 nm) .....	47
4.4.3 Results Obtained using Surface 3 (Ra=470 nm) .....	50
4.4 The Effect of Surface Preparation Method .....	53
The effect of the surface preparation method is discussed in this section considering each type of liquid used in this study. The images for the heater surface before and after boiling experiments using the three prepared surfaces are shown in Fig.4.13. ....	
4.4.1 Effect of Surface Preparation Method Observed from Distilled water Boiling Experiments .....	53
4.4.2. Nanofluids.....	57
4.4.3 Distilled Water on Nanofluids Deposited Surfaces.....	59
4.4.4 Nanosuspensions.....	61
Figure 4.21 Heat transfer coefficient for nanosuspensions on clean surface. ....	62
4.4.5 Distilled Water on Nanosuspensions Deposited Surfaces.....	63
4.4.6 SDBS and Distilled Water on Clean Surface.....	65
4.4 The Effect of the Transient Nature of the Nanoparticles Deposition Process.....	67
Chapter 5 Summary, Conclusion and Recommendations for Future Work.....	68
5.1 Summary and Conclusion .....	68
5.2 Recommendation for Future Work .....	70
Bibliography .....	71



## List of Figures

Figure 1.1 Boiling curve .[ <a href="http://www.thermalfluidscentral.org">http://www.thermalfluidscentral.org</a> ].	2
Figure 2.1 Boiling curves: (a) water , (b) F-77 [9].	7
Figure 2.2 Effect of surface roughness, particle size, and volume Concentration [14].	10
Figure 2.3 Images of nanoparticles layer forming on the heater surface from a single bubble (top) and the mechanism of the particle deposition during the boiling process (microlayer evaporation) [19].	13
Figure 2.4 Results of various studies in terms of the ratio of HTC of nanofluids to HTC of pure water obtained at different nanofluids concentrations.	16
Figure 3.1 The experimental setup.	19
Figure 3.2 The copper block.	20
Figure 3.3 Heater control circuit.	21
Figure 3.4 Location of the Zygo measurements of the boiling surface .	25
Figure 3.5 The profile of the boiling surface produced by diamond turning machine with average surface roughness of 6 nm .	26
Figure 3.6 The profile of the boiling surface produced by conventional lathe machine with average surface roughness of 470 nm.	26
Figure 3.7 The profile of the boiling surface produced by emery sandpaper with average surface roughness of 470 nm.	27
Figure 3.8 the experimental setup with the high speed imaging .	28
Figure 3.9 Measured temperature distributions at different heat flux inputs.	31
Figure 3.10 Actual particles' size using DLS: a) Nanofluids. B) Nanosuspensions .	35
Figure 4.1 Comparison between experimental data of boiling distilled water on surface 1 and data obtained using Rohsenow's correlation.	41
Figure 4.2 Repeatability test for distilled water boiling experiments using surface 1. ....	42
Figure 4.3 Repeatability test for nanosuspensions boiling experiments using surface 1.	42
Figure 4.4 Pool boiling curves obtained from boiling experiments performed using surface 1.	45
Figure 4.5 Heat transfer coefficient for different fluids using surface 1.	45
Figure 4.6 Images recorded during boiling experiments using surface 1, the heat flux for : Water: 1) 53.87 kW/m <sup>2</sup> , 2) 411.3 kW/m <sup>2</sup> , 3) 1126 kW/m <sup>2</sup> (CHF), Nanofluids: 1) 81.22 Kw/m <sup>2</sup> , 2) 405.5 kw/m <sup>2</sup> , 3) 940.6 kW/m <sup>2</sup> , Nanosuspensions: 1) 54.2 kW/m <sup>2</sup> , 2) 426.6 kW/m <sup>2</sup> , 3) 640 kW/m <sup>2</sup> (CHF).	46

Figure 4.7 Pool boiling curves obtained from boiling experiments performed using surface 2.....	49
Figure 4.8 Heat transfer coefficient for boiling experiments of different fluids on surface 2. ....	49
Figure 4.9 Images recorded during boiling experiments using surface 2. the heat flux for : Water: 1) 51 kW/m <sup>2</sup> ,2) 272.2 kW/m <sup>2</sup> , 3) 1322 kW/m <sup>2</sup> , Nanofluids: 1) 74.1 Kw/m <sup>2</sup> , 2) 280.8 kw/m <sup>2</sup> , 3) 807.8 kW/m <sup>2</sup> , Nanosuspensions: 1) 47.5 kW/m <sup>2</sup> , 2) 220.9 kW/m <sup>2</sup> ,3) 645 kW/m <sup>2</sup> . ....	50
Figure 4.10 Pool boiling curves obtained from boiling experiments performed using surface 3.....	52
Figure 4.11 Heat transfer coefficient for boiling experiments of different fluids on surface 3.....	52
Figure 4.12 Images recorded during boiling experiments using surface 3. the heat flux for : Water: 1) 47.1 kW/m <sup>2</sup> ,2) 391.1 kW/m <sup>2</sup> , 3) 938.7 kW/m <sup>2</sup> , Nanofluids: 1) 24.6 Kw/m <sup>2</sup> , 2) 267.9 kw/m <sup>2</sup> , 3) 384.9 kW/m <sup>2</sup> , Nanosuspensions: 1) 111 kW/m <sup>2</sup> , 2) 151 kW/m <sup>2</sup> ,3) 739 kW/m <sup>2</sup> . ....	53
Figure 4.13 Images taken for the various boiling surfaces. ....	54
Figure 4.14 Pool boiling curves obtained for distilled water on the three clean surfaces. .....	56
Figure 4.15 Heat transfer coefficient obtained for distilled water on the three clean surfaces. ....	56
Figure 4.16 Pool boiling curves obtained for nanofluids on the three clean surfaces. ....	58
Figure 4.17 Heat transfer coefficient obtained for nanofluids on the three clean surfaces. .....	58
Figure 4.18 Pool boiling curves for distilled water on nanofluids deposited surfaces (NFDS) . ....	60
Figure 4.19 Heat transfer coefficient for distilled water on nanofluids deposited surface(NFDS).....	60
Figure 4.20 Pool boiling curves obtained for boiling nanosuspensions on the three clean surfaces . ....	62
Figure 4.21 Heat transfer coefficient for nanosuspensions on clean surface. ....	62
Figure 4.22 Pool boiling curves obtained using distilled water on the three nanosuspensions deposited surfaces (NSDS) . ....	64
Figure 4.23 Heat transfer coefficient obtained from boiling curves of distilled water on nanosuspensions deposited surfaces (NSDS) . ....	64
Figure 4.24 Pool boiling curves obtained for boiling SDBS on the three clean surfaces .	66
Figure 4.25 Heat transfer coefficient for SDBS on clean surface.....	66
Figure 4.26 Heater Surface fluctuations during the test. ....	67

## **List of Tables**

Table 3.1 Summary for the calculated uncertainties.....	33
Table 3.2 Details of the experiments performed using the three prepared surfaces .....	39
Table 4.1 Details of pool boiling experiments performed on surface 1 ( Ra=6 nm).....	43
Table 4.2 Details of pool boiling experiments performed on surface 2 (Ra = 470 nm). ...	48
Table 4.3 Details of pool boiling experiments performed on surface 3 (Ra = 470 nm). ...	51
Table 4.4 Details of surface measurements performed on all three clean surfaces after preparation. ....	55
Table 4.5 Results of surface measurements performed before and after nanofluids boiling experiments. ....	59
Table 4.6 Results of surface measurements performed before and after nanosuspensions boiling experiments.....	63

## Nomenclature

SYMBOL	DESCRIPTION	UNITS
$C_p$	<i>Specific heat</i>	$J/Kg^{\circ}C$
$C_{sf}$	<i>Surface fluid combination factor</i>	-
$g$	<i>Gravitational acceleration</i>	$m/s^2$
$h$	<i>Heat transfer coefficient (HTC)</i>	$W/m^2^{\circ}C$
$h_{lv}$	<i>Latent heat of vaporization</i>	$J/kg$
$k$	<i>Thermal conductivity</i>	$W/m^{\circ}C$
$q''$	<i>Heat flux</i>	$W/m^2$
$R_a$	<i>Average surface roughness</i>	$m$
$rms$	<i>Root mean square</i>	$m$
$R_z$	<i>Ten points heights</i>	$m$
$PV$	<i>Maximum peak to valley height</i>	$m$
$SIP$	<i>Surface interaction parameter</i>	-
$T$	<i>Temperature</i>	$^{\circ}C$
$L$	<i>Displacement</i>	$m$

<b>Greek Symbols</b>		
SYMBOL	DESCRIPTION	UNITS
$\mu$	<i>Viscosity</i>	$Ns/m^2$
$\rho_l$	<i>Liquid density</i>	$kg/m^3$
$\sigma$	<i>Surface tension</i>	$N/m$

### Subscripts

$f$	<i>Fluid</i>
$v$	<i>Vapor</i>
$w$	<i>Water</i>
$NF$	<i>Nanofluids</i>
$NS$	<i>Nanosuspension</i>
$NFDS$	<i>Nanofluids deposited surface</i>
$NSDS$	<i>Nanosuspension deposited surface</i>
$SDBS$	<i>Sodium dodecylbenzenesulfonate</i>
$sat$	<i>Saturation</i>
$s$	<i>Surface</i>
$wt$	<i>Weight</i>

## **Chapter 1 Introduction**

Boiling is a complex phenomenon involved in many industrial applications because of its ability to remove high rates of heat. The process is represented by the vapor bubbles formation that grow and detach from the heated surface. Moreover, the dynamic of these vapor bubbles depend on the surface and liquid temperature, surface characteristics, and the thermo-physical properties of the liquid [1].

### **1.1 Pool Boiling**

Boiling that occurs when the heating surface is submerged in a quiescent liquid is referred to as Pool boiling [2]. Nukiyama [3] was the first to introduce that boiling can be characterized by four regimes: natural convection, nucleate boiling, transition boiling, and film boiling, as shown by the boiling curve indicated in Fig1.1.

#### **1.1.1 Natural Convection**

The natural convection regime or free convection is up to point A, the surface superheat is low enough that nucleation sites are not active and heat at the surface is removed by single phase natural convection to the fluid and there is no bubble formation on the heated surface.

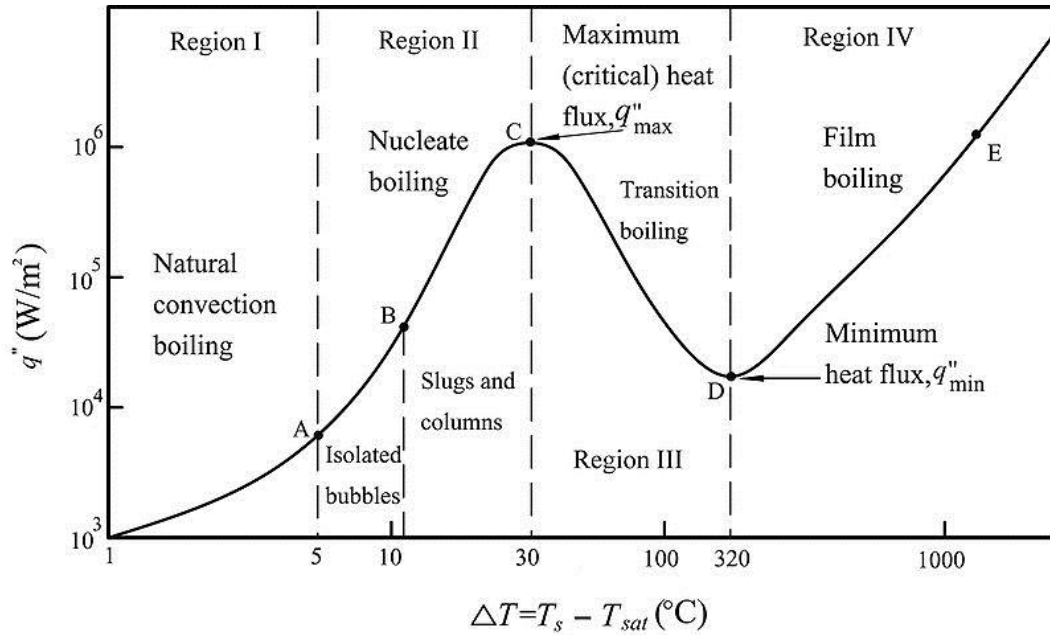


Figure 1.1 Boiling curve .[ <http://www.thermalfuidscentral.org>]

### 1.1.2 Nucleate Boiling

The Nucleate boiling regime spans between points A and C, in which the surface superheat is high enough so that the nucleation sites are active, bubbles form and detached from the heated surface independently (point A to point B). Then, as the surface superheat rises beyond point B, more nucleation sites are becoming active and bubbles start to interact and merge to form large bubbles that release higher heat flux. Finally, at certain surface superheat, the heat flux reaches a maximum value, called the critical heat flux (CHF), after which vapour batches prevent the liquid from touching the heated surface, causing the heat flux to decrease rapidly reaching its minimum value. In power controlled systems,

enormous increase in the wall superheat leads to point E causing severe damage to the heated surface.

The nucleate boiling regime is the favorable regime used in many industrial applications because of its ability to remove high rates of heat. Applications are too many such as cooling systems of nuclear reactors and cooling of modern electronic devices.

### **1.1.3 Transition Boiling**

Transition boiling can be observed clearly in the temperature controlled boiling systems. It is between point C and point D in which case the heated surface is covered by an unstable vapor layer.

### **1.1.4 Film Boiling**

Film boiling occurs between points D and E in which case the heated surface is totally covered by a stable vapor layer. Film boiling can be observed only in temperature controlled boiling systems.

## **1.2 Nanofluids**

Nanofluids are suspended solid nanoparticles in a base fluid. One well known example of nanofluids that is used by many researchers is water based alumina oxide nanofluids in which alumina oxide nanoparticles are dispersed in water.

The term “nanofluids” has been introduced first by Choi [4] in 1995 followed by many interests from researchers worldwide who studied the thermo-physical properties of nanofluids as well as their ability to work as working fluids in heat transfer applications. However, enhancing the thermal conductivity of a liquid by dispersing solid particles was proposed by Maxwell in 1873 [5]. Settlement, erosion, clogging and pressure drop caused by large-sized solid particles limited the use of such suspensions for a long time [6].

To understand the effect of nanofluids on the rate of heat transfer, many theoretical and experimental studies have been carried out considering different parameters such as: volume concentration [7, 8, 9], nanoparticles size and material [9, 8], as well as type of base fluid [10, 11].

Studies on boiling of nanofluids have shown contradicting results. Some investigations reported enhancement and others reported deterioration in the rate of heat transfer with respect to pure water [12]. A number of experimental studies of pool boiling of nanofluids, including the present one, have been carried out at the Thermal Processing laboratory at McMaster University trying to understand the possible reason(s) for these contradicting results.



## Chapter 2 Literature Review and Research Objectives and Plan

Section 2.1 of this chapter presents a literature review of the effect of heater surface condition on boiling heat transfer of pure liquids. Section 2.2 includes a review of the most important works that have been carried out on pool boiling of nanofluids. Section 2.3 discusses the mechanism of nanoparticles deposition that has been observed during pool boiling of nanofluids. The effect of particles deposition is discussed in section 2.4. Section 2.5 provides a summary of the experimental results of the investigations discussed in sections 2.2, 2.3 and 2.4. Research objectives and plan and thesis structure are presented in sections 2.6 and 2.7, respectively.

### 2.1 Effect of Surface Condition on Boiling Heat Transfer of Pure Liquids

The effect of the surface roughness on the rate of heat transfer has been investigated by many researchers. The average surface roughness ( $R_a$ ), root mean square (rms), mean total roughness ( $R_z$ ) as well as the way of the surface treatment are amongst the common parameters considered in those studies. Generally speaking, the shape and size of the cavity with the surface wettability are the main parameters that determine the number of active nucleation sites [13].

A well-known correlation that predicts the heat transfer coefficient (HTC) in nucleate boiling regime is the one proposed by Rohsenow [1], which is given by equation (2.1)

$$q_s'' = \mu_l h_{fg} \left[ \frac{g(\rho_l - \rho_v)}{\sigma} \right]^{1/2} \left( \frac{C_{p,l}(T_s - T_{sat})}{C_{s,f} h_{fg} Pr_l^n} \right)^3 \quad (2.1)$$

Which  $q''$  is the heat flux,  $\mu$  is the liquid viscosity,  $h_{fg}$  is the latent heat of vaporization,  $\sigma$  is the surface tension,  $g$  is the acceleration due to gravity,  $\rho_l$  is the liquid density,  $\rho_g$  is the vapor density,  $C_{p,l}$  is the liquid specific heat,  $T_s - T_{sat}$  is the wall superheat,  $n$  is constant that depends on the fluid type,  $Pr_l$  is the Prandtl number for the liquid and  $C_{s,f}$  is an arbitrary surface constant that depends of the surface to liquid combination.

Kang [14] conducted an experimental study using a tubular heat exchanger to determine the effect of surface roughness on saturated pool boiling heat transfer of water at atmospheric pressure. Boiling curves have been experimentally obtained using various combinations of tube diameters ( $D = 9.7, 19.05, \text{ and } 25.4$  mm), heating surface roughness (rms= 15.1 and 60.9 nm), tube orientations ( $\theta=0^\circ, 45^\circ, \text{ and } 90^\circ$ ), and tube lengths ( $L = 100, 300, \text{ and } 530$  mm). He concluded that for the horizontal tube, the increase in surface roughness gives no credible change in heat transfer, particularly at high heat fluxes. On the other hand, the effect of surface roughness was more pronounced as the orientation of the heater tube changes from horizontal to vertical. . The author attributed his results to the enhancement in liquid agitation and bubble coalescence associated with the change in tube orientation from horizontal to vertical.

Jones et. al. [15] experimentally investigated the influence of surface roughness on nucleate pool boiling heat transfer of water and Fluorinert F-77 on flat and horizontal aluminum surface. They considered a wide range of average surface roughness values. They prepared their surfaces using emery paper (polished) and electrical discharge machining (EDM). The surface roughness ranged from  $R_a = 0.027 \mu\text{m}$  to  $0.038 \mu\text{m}$  for the polished surfaces and from  $1.08 \mu\text{m}$  to  $10.0 \mu\text{m}$  for the EDM surfaces. Their results showed that for the FC-77, the heat transfer coefficient (HTC) was continually increasing with increasing the surface roughness. For water, however, EDM surfaces of intermediate roughness ( $R_a = 1.08, 2.22, \text{ and } 5.89 \mu\text{m}$ ) did not show a significant change in the HTC that was higher than the polished surface of  $R_a = 0.038 \mu\text{m}$ . The roughest EDM surface ( $R_a = 10.0 \mu\text{m}$ ) showed the highest heat transfer coefficient. Part of their results is shown here in Fig.2.1.

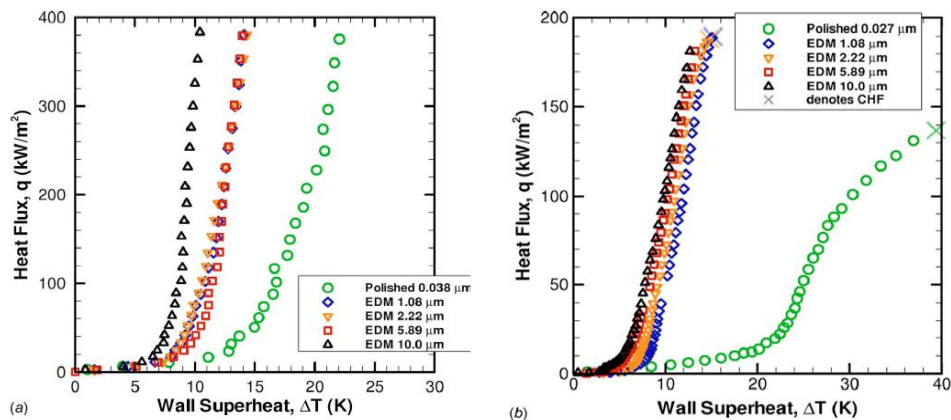


Figure 2.1 Boiling curves: (a) water , (b) F-77 [9].

## 2.2 Investigations carried out on Pool Boiling of Nanofluids

Taylor et.al. [16] reviewed recent studies of pool boiling of nanofluids and showed the reported contradicting trends about whether nanofluids can enhance or deteriorate boiling heat transfer. Most studies reported fouling of the boiling surface from the deposition of nanoparticles. They concluded that nanoparticles deposition has a significant effect on the heat transfer performance of nanofluids.

Das et. Al. [17] conducted an experimental study of pool boiling of water– $\text{Al}_2\text{O}_3$  nanofluids on a horizontal cartridge heater of 20 mm diameter. Using emery sandpaper, they produced boiling surfaces with two different  $R_a$  values, 0.4  $\mu\text{m}$  and 1.15  $\mu\text{m}$ . Nanoparticles volume concentration was varied between 1% and 4%. They prepared their nanofluids from dry powder. They found that the increase in the nanoparticles concentration results in more deterioration in the HTC with respect to pure water. They concluded that the change of surface characteristics during boiling due to the trapped nanoparticles is the reason of this deterioration since the nanoparticles were an order or two orders of magnitude smaller than that of the average surface roughness.

Bang and Chang [18] performed pool boiling of alumina-water nanofluids with 0.5, 1, 2, and 4% volume concentrations on a 4x100 mm rectangular heater with a 1.9 mm thickness. The boiling surface has been prepared by using emery sandpaper to produce a smooth surface of  $R_a = 37$  nm. It has been found that the addition of alumina nanoparticles caused a decrease in the number of nucleation

sites, and therefore a decrease in the heat transfer coefficient. However, the critical heat flux (CHF) was enhanced for both the horizontal flat surface and vertical flat surface by  $\sim 32\%$  and  $\sim 13\%$ , respectively. The authors concluded that the nanoparticles reduced the number of nucleation sites and liquid was trapped near the surface within the porous nanoparticles layer, which caused an enhancement in the CHF.

Vassallo et. al. [12] conducted pool boiling experiments of silica-water nanofluids of 0.5 % volume concentration on a 0.4 mm diameter and 75 mm long NiCr wire with nanoparticles size of 15 and 50 nm. No enhancement was found in the nucleate boiling regime, instead, an increase in the CHF was observed for both nanoparticles sizes. Moreover, in the case of the larger particles size, the heating wire did not fail and was able to work under the maximum power. A coating layer was observed on the wire following the boiling experiments. To examine the effect of the particles size,  $3 \mu\text{m}$  silica particles with a volume concentration of 0.5 % were tested. Regardless of the low dispersion of the large particles, a significant increase in the CHF was attained.

Narayan et. al. [9] carried out experiments by using stable water based nanofluids containing alumina nanoparticles of average sizes of 47 and 150 nm. They used a vertical tubular heater of various surface roughness ( $R_a = 48, 98, \text{ and } 524 \text{ nm}$ ) prepared by using emery sandpaper. They observed an enhancement in

the HTC up 70% for the rough heater of  $R_a=524$  nm and 0.5 % mass concentration. For the smooth heater with  $R_a=48$  nm, remarkable deterioration and reduction in the HTC by nearly 45% was found at particle mass concentration of 2 %. In order to explain their contradicting results, they proposed a new parameter called the surface interaction parameter (*SIP*) defined as the ratio of the average particle size to the average surface roughness of the heater. They hypothesised that when the *SIP* is near unity, the heat transfer coefficient decreases, as in the case of the smooth surface ( $R_a=48$  nm) and the 47 nm nanoparticles,  $SIP = 1.02$ . However, if the *SIP* is far from unity, then the HTC increases, as in the case of surface roughness  $R_a= 524$  nm and nanoparticles size of 47 nm,  $SIP = 10.38$ , see Fig.2.2.

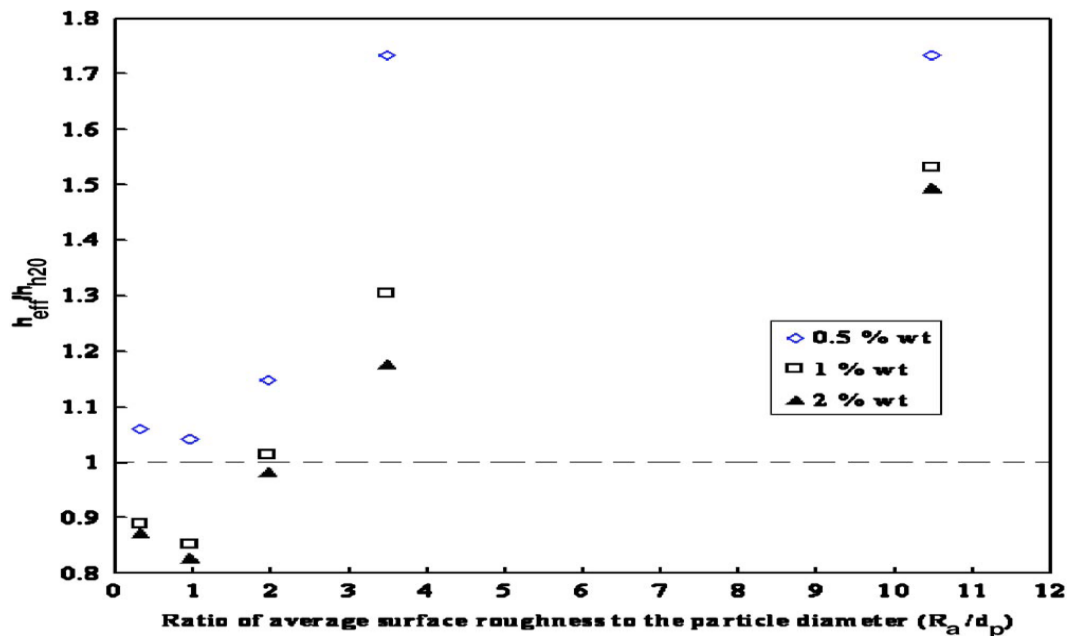


Figure 2.2 Effect of surface roughness, particle size, and volume Concentration [14].

Harish et. al. [7] studied the effect of surface particle interactions during pool boiling of nanofluids on a 314 mm<sup>2</sup> aluminum disc. In this study, Alumina oxide 50 nm particles were dispersed in double distilled water at 0.5, 1, and 2 % volume concentrations. The nanofluids were stabilised by making them slightly acidic with pH at 4.5. The heater surface was polished by using emery sandpaper and a lapping machine operating at 1300 rpm to produce a smooth surface with  $R_a=53\pm 12.5$  nm and a rough surface with  $R_a=308 \pm 5.7$  nm. For the rough heater, their results showed an enhancement in the boiling heat transfer with volume concentration 1% and 2%. The results for the 0.5 %Vol. and 1 %Vol. concentrations were nearly the same. For the smooth heater, on the other hand, their results showed a deterioration of approximately 20%, 26% and 30% at volume concentrations of 0.5%, 1% and 2%, respectively. They concluded that nanoparticles at different values of the *SIP* can either split or plug of the surface cavities, thereby enhancing or deteriorating the boiling heat transfer.

Wen et. al. [19] experimentally studied the effect of the heating surface modification on pool boiling of alumina-water nanofluids. The boiling surfaces were made of brass and have a rectangular shape with two values of average surface roughness of  $R_a=420$  nm for the rough surface and  $R_a= 25$  nm for the smooth one. They used only 0.001 % Vol. concentration with an initial particles size of 20 – 150 nm. They measured the actual nanoparticles size using a dynamic light scattering instrument and found it to be between 150 – 900 nm with an average value of 405 nm. Their results are opposite to those reported in [9] in

which case the smooth surface resulted in an enhancement in the HTC due to the increase in the surface roughness. The rough surface showed no obvious change in the heat transfer performance. They concluded that the performance of boiling heat transfer of nanofluids is dependent upon the relative size between the actual particles size and the heating surface geometry and their interaction.

Abdelhady [8] reported results of a set of experiments of pool boiling and jet impingement boiling of  $\text{Al}_2\text{O}_3$ -water based nanofluids conducted using a flat copper surface polished by using emery sandpaper. In the pool boiling experiments, Abdelhady investigated the effect of surface roughness ( $R_a = 20, 80,$  and  $420 \text{ nm}$ ), particles concentration (0.005 and 0.01% Vol.), particles size (10, and 50 nm) as well as nanoparticles material ( $\text{Al}_2\text{O}_3$  and CuO). The author concluded that the *SIP* parameter that has been introduced by G. Prakash Narayan [9] cannot be used to describe the discrepancy in the boiling heat transfer results. However, Abdelhady attributed his results to the overall nanoparticles deposition on the heater surface. He observed enhancements in the heat transfer coefficient when the nanoparticles deposition pattern covered less than 90% of the heater surface, while, deteriorations in the HTC were observed when the deposition pattern covered than 90% of the heater surface.

### **2.3 The Mechanism of Nanoparticles Deposition**

Nanoparticles deposition has been reported by many researchers [16]. The mechanism responsible for the nanoparticles deposition has been discussed by



Kim et. al. [20] that nanoparticles deposition is due to microlayer evaporation. Kwark et. al. [21] confirmed this mechanism experimentally. They carried out boiling experiment of alumina nanofluids at 1 g/l on a copper heater. They increased the power to the heater until one bubble initiated and left it for 2 minutes under these conditions. After removing the heater from the setup, they observed a deposition layer formed only at the active nucleation site, as shown in Fig 2.3 .

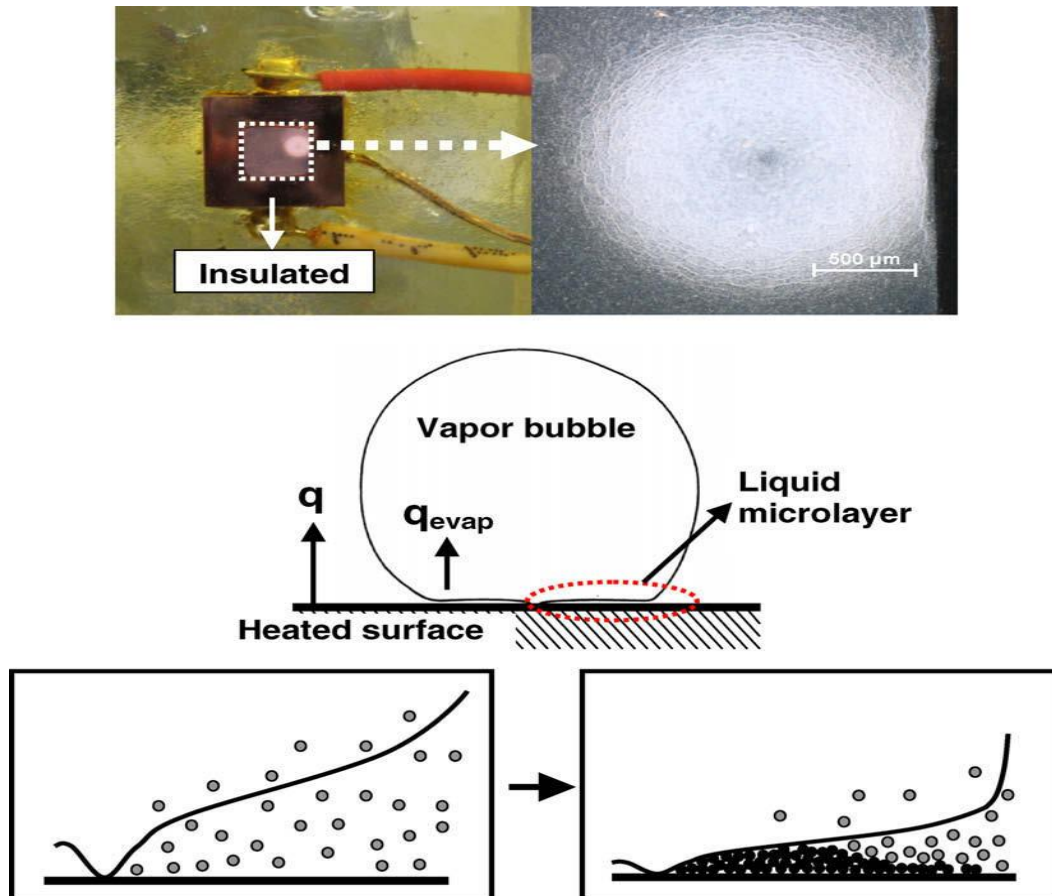


Figure 2.3 Images of nanoparticles layer forming on the heater surface from a single bubble (top) and the mechanism of the particle deposition during the boiling process (microlayer evaporation) [19].

Moreover, microlayer evaporation increases the concentration of the nanoparticles in the liquid microlayer region and decreases the distance between the nanoparticles so that the possibility of collision, agglomeration and eventually deposition of the nanoparticles on the heated surface increases [22].

#### **2.4 Effect of Nanoparticles Deposition on the Boiling Surface**

Pool boiling experiments performed by means of nanofluids as a working fluid showed changes in the surface roughness due to nanoparticles deposition. It has been reported that this coating layer is a contributing factor in changing the heat transfer performance observed during nanofluids boiling [23]. Also, some researchers hypothesized that the enhancement of the heat transfer coefficient that could be achieved by nanofluids is due to the ability of the deposited nanoparticles to settle in cavities and multiply the number of nucleation sites [9].

In a study performed by Coursey and Kim [24] to investigate the effect of surface wettability of boiling nanofluids. The surface energy was measured by measuring the advancing three-phase contact angle. They changed the alumina oxide nanoparticle concentrations from 0.001 g/L to 10 g/L. Their results with the 0.5 g/L showed up to 37% enhancement in the CHF. They concluded that the addition of nanoparticles to water improved surface wetting, but only when the surface was fouled by the nanoparticles.

Ahmed and Hamed [25] conducted a set of pool boiling experiments of alumina-water based nanofluids with initial particle size of 40-50 nm. They used a horizontal flat copper surface. They used nanofluids at concentrations of 0.01, 0.1

and 0.5 vol.%. Pure water experiments were performed on the nanoparticle-deposited (NPD) surfaces. Their results showed that boiling of pure water on the NPD surface produced by the highest concentration nanofluids experiments resulted in the highest HTC. The authors proposed different values of the transient surface factor in Rohsenow correlation ( $C_{sf}$ ) to account for the transient nature of the nanoparticles deposition at different volume concentrations. Such deposition could reduce the number of active nucleation sites as well as acts as an insulation layer on the surface. They concluded that the deposited layer happened at a slower rate in the case of low nanofluids concentration (0.01 vol.%) resulting in an enhancement in the rate of heat transfer which was attributed to the effect of the higher thermal conductivity of nanofluids being more dominant than the effect of nanoparticles deposition on the surface. Also, nanoparticles deposition could reduce the number of active nucleation sites and works as an insulation layer on the surface .

## **2.5 Summary and Objectives of the Present Study**

Fig. 2.4 presents the ratio of pool boiling HTC of nanofluids to the HTC of pure water obtained at different nanofluids concentrations reported by various researchers. One can easily note the clear contradiction in these findings. In general, large volume (>2 % Vol.) concentrations of nanoparticles showed deterioration as reported by [17, 18]. On the other hand, some researchers reported enhancement and deterioration in the HTC of nanofluids , [9, 7], while others reported no change [19, 21]. It should be noted that most of these

researchers signified the importance of surfaces nanoparticles interaction during nanofluids pool boiling experiments. Most of these experiments have been conducted using different initial boiling surface conditions using surfaces that were mostly prepared using sandpaper polishing. The effect of heater surface preparation method has not been widely investigated.

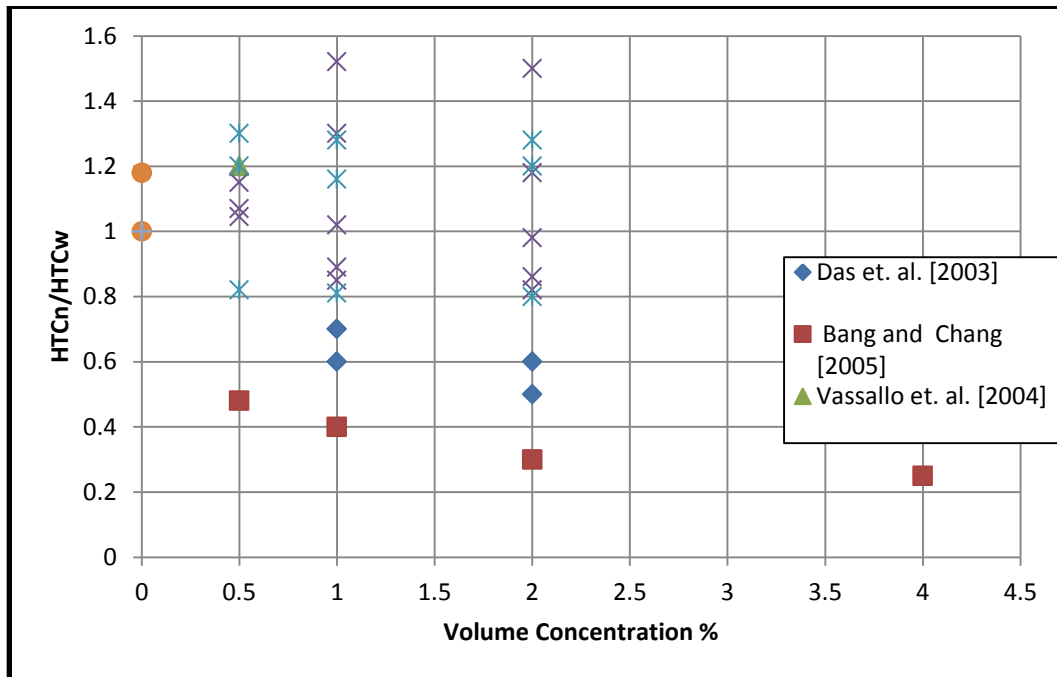


Figure 2.4 Results of various studies in terms of the ratio of HTC of nanofluids to HTC of pure water obtained at different nanofluids concentrations.

As surfaces produced in the industry using various methods and at various levels of smoothness, the focus of this study is to:

1. investigate the effect of surface smoothness at a level that has not been investigated before, and
2. investigate the effect of the method heater surface preparation on the rate of heat transfer during pool boiling of nanofluids

Therefore, the experimental work in this study has been carried out in two stages:-

Stage 1: A set of pool boiling experiments were carried out on an ultra-smooth and consistent surface that had an average surface roughness of the same order of magnitude as of the initial nanoparticles size.

Stage 2: investigate the effect of the method of heater surface preparation on the pool boiling of nanofluids, while maintaining the same initial average surface roughness of the heater surface. In this study, nanofluids have been prepared from  $\text{Al}_2\text{O}_3$  nanoparticles and pure distilled water. Nanoparticles deposition has been observed to have a less effect at low concentrations, therefore, in this study, a low concentration of 0.05% by mass (0.0012% Vol.) has been used and kept constant throughout the present investigation. The boiling surface used in the present study is a flat horizontal copper surface prepared by using three different preparation methods. More details will be provided in the subsequent chapters.

## **2.7 Thesis Structure**

Chapter 3 provides details of the experimental facilities and methodology. Chapter 4 presents validation of the experimental setup, repeatability and all experimental results. Chapter 5 includes the summary ,main conclusions and recommendations for future work.

## Chapter 3 Experiments Setup and Methodology

This chapter presents the experimental setup and methodology used for the experimental investigation. The details and specifications of the hardware are provided in detail in section 3.1. Thermocouples calibration is presented in section 3.2. Section 3.3 presents surface roughness measurements followed by a detail of the surface preparation methods used in the study in section 3.4. High speed imaging setup is represented in section 3.5. The determination of surface heat flux and surface temperature are discussed in section 3.6 followed by a detailed section on uncertainty analysis in section 3.7. Nanofluids preparation method is represented in section 3.8 followed by the experiment procedures in section 3.9. Section 3.10 concludes with the parameters investigated throughout the experiments.

### 3.1 Experimental Setup

The experimental setup used in this study is shown in Figure 3.1. A vessel made of stainless steel with 20 cm diameter stainless steel is the main body of the setup (13). A stainless steel skirt is fixed (16) to support the liquid within the vessel. The boiling surface is a 25.4 mm diameter and 71 mm length copper block (18) that is installed at the centre of the skirt. Three  $\frac{1}{4}$  inch diameter and 1  $\frac{1}{2}$  inch length cartridge heaters are fixed inside the bottom of the copper block to heat up the copper block, referred to as the Main Heaters (8). The maximum power of the main heaters is 750 W which is capable of providing a maximum

heat flux of  $1.48 \text{ kW/m}^2$ . Three 1.0 mm diameter type-E thermocouples (17) are installed in the copper block at different axial distances from the top of the block to determine the axial temperature profile of the copper block.

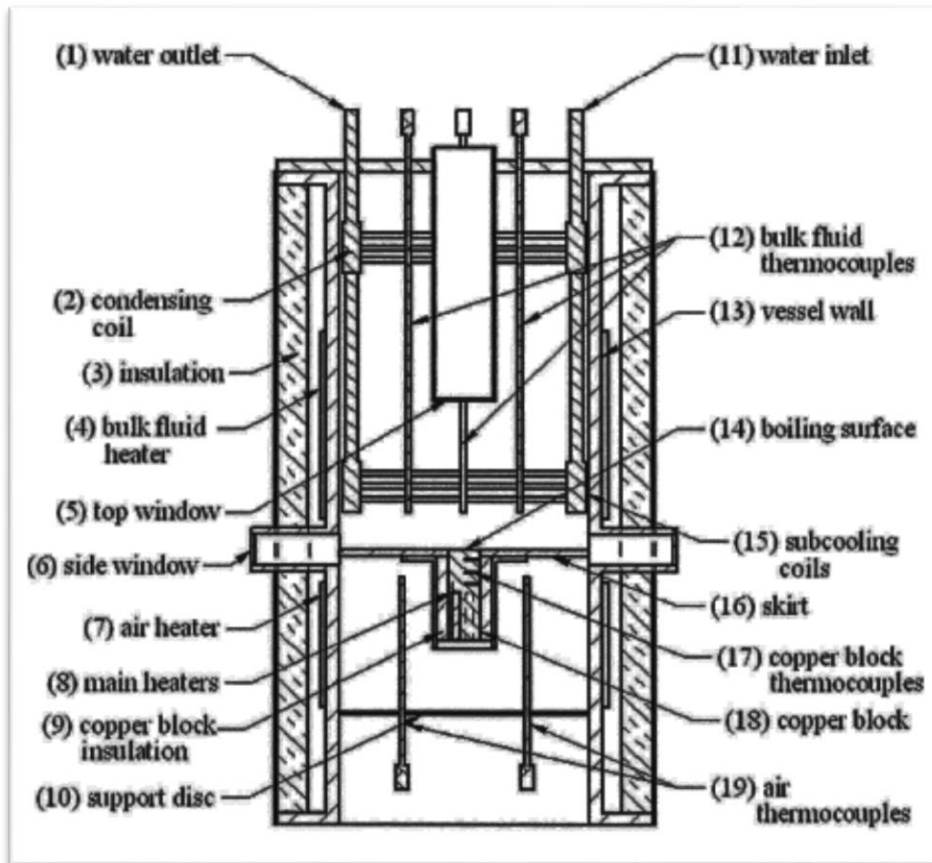


Figure 3.1 The experimental setup.

The locations of the thermocouples in the copper blocks are shown in Figure 3.2. The copper block is wrapped in insulation (9) to reduce radial heat losses. Two heaters are installed around the outside of the vessel wall with a combined power of 3000 W to heat up the liquid to saturation temperature, referred to as Bulk Fluid Heaters (4). Two 3.2 mm diameter type-E thermocouples were immersed in

the bulk fluid to record its temperature (12). Another heater is installed around the copper block to heat the surrounding air to reduce radial heat losses, referred to as Air Heater (7).

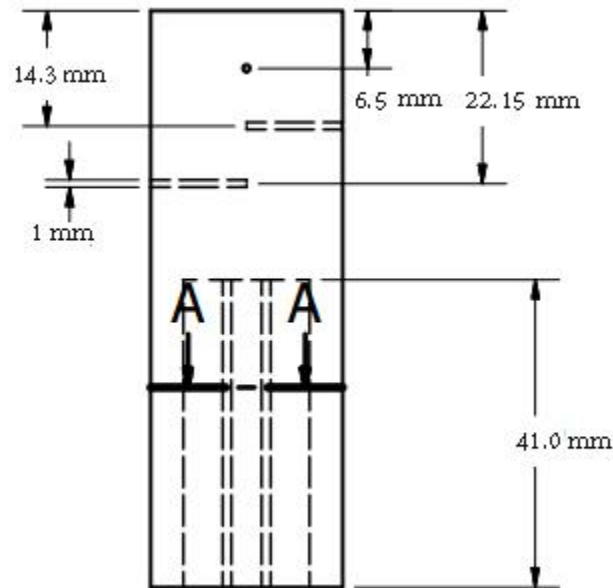


Figure 3.2 The copper block.

A support disc (10) is used to trap the air around the copper block to minimise mixing with the air in the room. A thermocouple (19) is installed to monitor the air temperature around the copper block. A condensing coil (2) is used to minimise the loss of fluid and maintain a constant concentration throughout the experiment time when boiling nanofluids. The water flow rate through the condensing coil is regulated through a needle valve. A heater is installed in the inlet condensing water pipe to heat up the inlet condensing water and prevent sub-cooling to take place. A thermocouple is installed to monitor the temperature of



the inlet condensing water, as well as a flow meter to measure its flow rate. A sub-cooling coil (15) is used to lower the liquid temperature before it was drained out of the vessel. Two opposing glass side windows (6) allow visual observation of the boiling phenomenon on the surface from the side. A top window (5) also allows visual observation of the boiling surface from above. The diameters of the side windows are 2.5 cm and the top window is 4.5 cm. The whole vessel is wrapped with an aluminium cover to protect the user from contacting the heaters. Insulation (3) is attached between the cover and the vessel to reduce heat losses from the vessel and conserve power.

### 3.1.1 Heaters Control

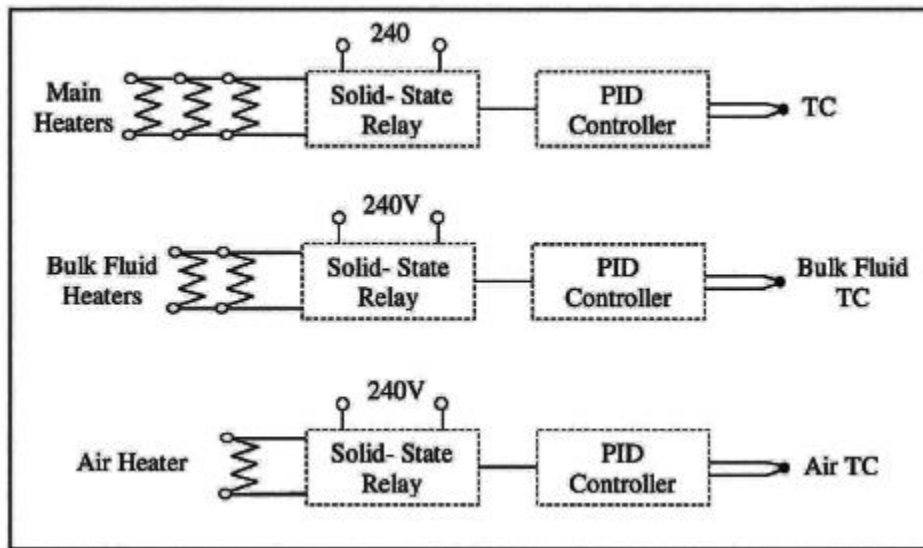


Figure 3.3 Heater control circuit.

The three heaters used in this study have been controlled by ON/OFF PID controllers from Watlow as schematically shown in Fig 3.3. The air and bulk fluid temperature, are measured using two thermocouples to feed the PID

controllers to feed the Air Heater and Bulk Fluid Heater in order to achieve the desired temperatures. For the Main Heater, it is desired to have a controlled heat flux boiling experiments. Therefore, the Main Heater is controlled in the manual mode by varying the input power to increase or decrease the heat flux. Additionally, a dead thermocouple has been connected to the Main Heater to feed the PID controller, otherwise an error will be displayed and the controller will not work.

### **3.1 .2 Data Acquisition**

The thermocouples are connected to a Kiethley Data Acquisition System Model 2700 and then to a personal computer. Temperatures are recorded using ExceLinx software that is installed into Microsoft Excel on the computer. The temperatures are scanned once every 5 seconds for the following thermocouples:

- Three axial locations in the copper block
- two bulk liquid locations
- air around copper block
- water heater
- air heater
- inlet condensing water

### **3.2 Thermocouple Calibration**

The thermocouples used in the experiments were calibrated against a high-precision resistive temperature detector (RTD) probe (Omega DP251 precision

RTD thermometer with PRP-3 probe). The accuracy in this system is  $0.025^{\circ}\text{C}$  in a range of  $-50^{\circ}\text{C}$  to  $250^{\circ}\text{C}$ . The sheathed thermocouple probes were submerged in a well-insulated and heated oil bath with the temperature monitored by the RTD. The power of the heater was controlled gradually and the RTD and thermocouple temperature readings were recorded. The oil bath was assumed to be at a uniform temperature because of its small volume. A least squares was used to fit each data set (thermocouple reading versus RTD reading). The resulting relationship was used to relate thermocouple measurements (y) to calibrated temperatures (x).

### **3.3 Surface Roughness Measurements**

The surface measurements has been done optically using a Zygo NewView 5000 white-light interferometer. It is a microscope has a 20X internal magnification mounted on a granite base and stable gantry column. Three objective lens of 1X, 10X, and 50X can be used to have magnification from 0.4 to 2.0. The microscope is also equipped with a 4 axis stage with X and Y linear axes with roll and pitch. This microscope is then connected to a personal computer that has CCD camera having a resolution of 640x480 pixels. The Zygo Corporation also provides the MetroPro software for analyzing the scanned surface.

In this study, the surface finish measurements was performed using 10X objective lens to scan area of  $0.36\text{ mm} \times 0.27\text{ mm}$  for five locations of the surface as seen is Fig.3.4. The following parameter can be measured using the Zygo software :

1- Average surface roughness ( $R_a$ ) : The arithmetic average of the absolute values of the roughness profile. It can be calculated as :

$$R_a = \frac{1}{L} \int_0^L |z(x) dx| \quad (3.1)$$

2- Root mean square (rms) : The average of the measured height deviations taken within the evaluation length or area and measured from the mean linear surface. It can be calculated as follow :

$$rms = \sqrt{\frac{1}{L} \int_0^L z^2(x) dx} \quad (3.2)$$

3- Ten points heights ( $R_z$ ) : The average absolute value of the five highest peaks and the five lowest valleys over the evaluation length. It can be calculated as follow :

$$R_z = \frac{(P1 + \dots + P5) - (V1 + \dots + V5)}{5} \quad (3.3)$$

4- Maximum peak to valley height (PV) : The absolute value between the highest and lowest peaks. It can be calculated as follow :

$$PV = R_p + R_v \quad (3.4)$$

### 3.4 Surface Preparation

#### 3.4.1 The Ultra Smooth Surface, Prepared Using a Diamond Turning Machine

A diamond turning machine, model 700G from Precitech Freeform, has been used to produce an ultra-smooth surface ( mirror finish). This machine is a high

performance, ultra- precision machine with a computer numerical control that uses a single diamond crystal (SDC) tool. It is suitable for the production of

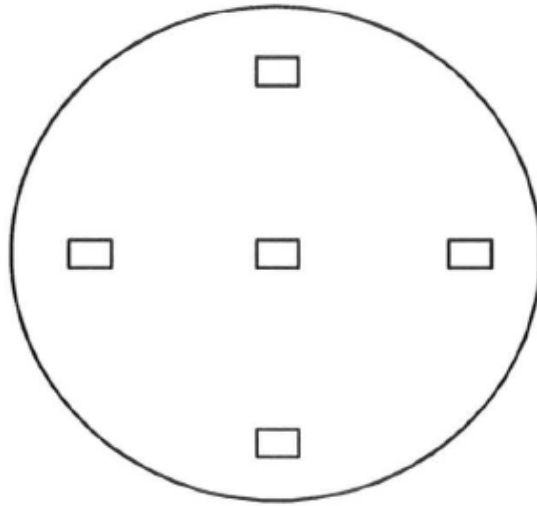


Figure 3.4 Location of the Zygo measurements of the boiling surface .

optical and mechanical components. The machine tool has three linear axes (X, Y, Z) as well as one rotational axis. In order to produce a mirror surface with  $6\pm 3$  nm average roughness, the copper block was diamond turned at 1000 RPM with a feed rate of  $5 \mu\text{m}/\text{rev}$  and a depth of cut of  $2 \mu\text{m}$  . The copper surface was scanned using the Zygo as seen is Fig. 3.5 .

### 3.4.2 Rough Surface 1, Prepared using a Conventional Lathe Machine

The conventional lathe machine has been used to produce a rough surface with an average surface roughness of  $470\pm 30$  nm. In this case, the copper surface was machined at 820 RPM with a feed rate of 3.6 thou/rev ( $91.44 \mu\text{m}/\text{rev}$ ) and

depth of cut of 10 thou ( $254 \mu\text{m}$ ). The copper surface was then scanned using the Zygo as shown in Fig.3.6.

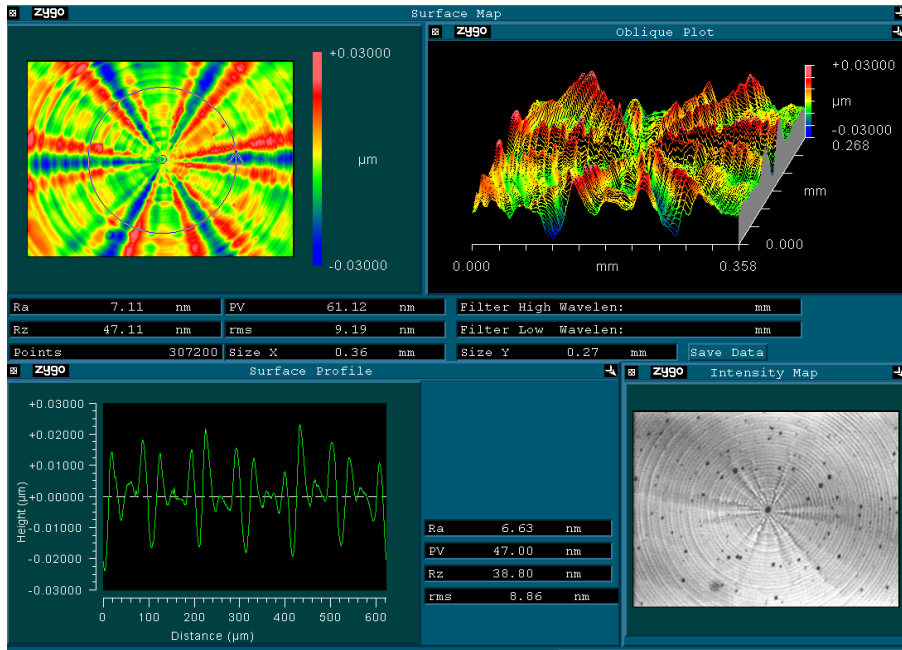


Figure 3.5 The profile of the boiling surface produced by diamond turning machine with average surface roughness of 6 nm .

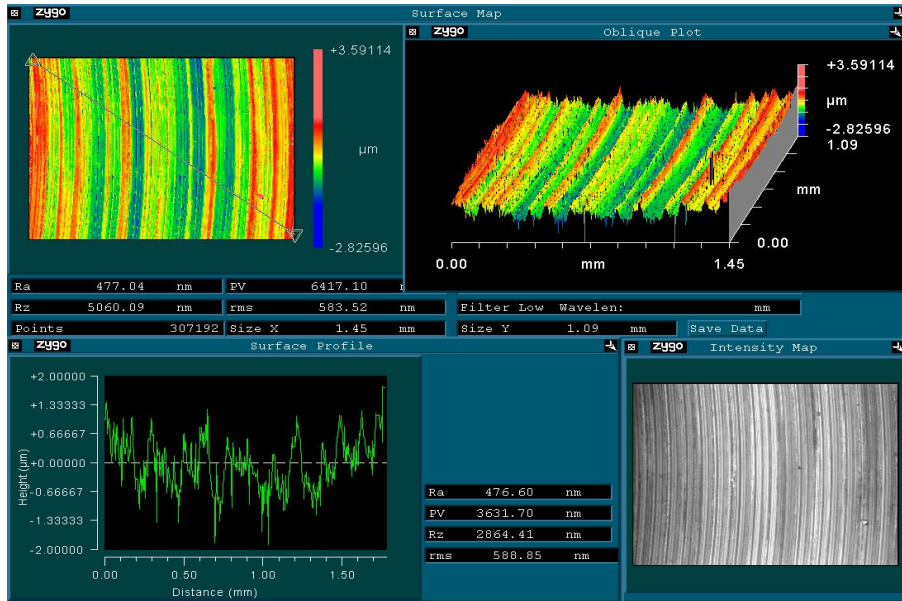


Figure 3.6 The profile of the boiling surface produced by conventional lathe machine with average surface roughness of 470 nm.

### 3.4.3 Rough Surface 2 prepared using Emery Sandpaper

In order to investigate the effect of the method of heater surface preparation, a polished surface has been produced using emery sandpaper. In this case, the copper block was held by hand under the effect of its weight while the surface was downward facing wet sandpaper. The copper block was then moved back and forth under these conditions for 1 minute before it was turned 90° and polished again for the same time. The same procedure was repeated using silicon carbide emery sandpaper of grit P180 followed by grit P320 to achieve the desired roughness. The surface roughness was then determined from the scanned surface using the Zygo machine, as shown Fig.3.7.

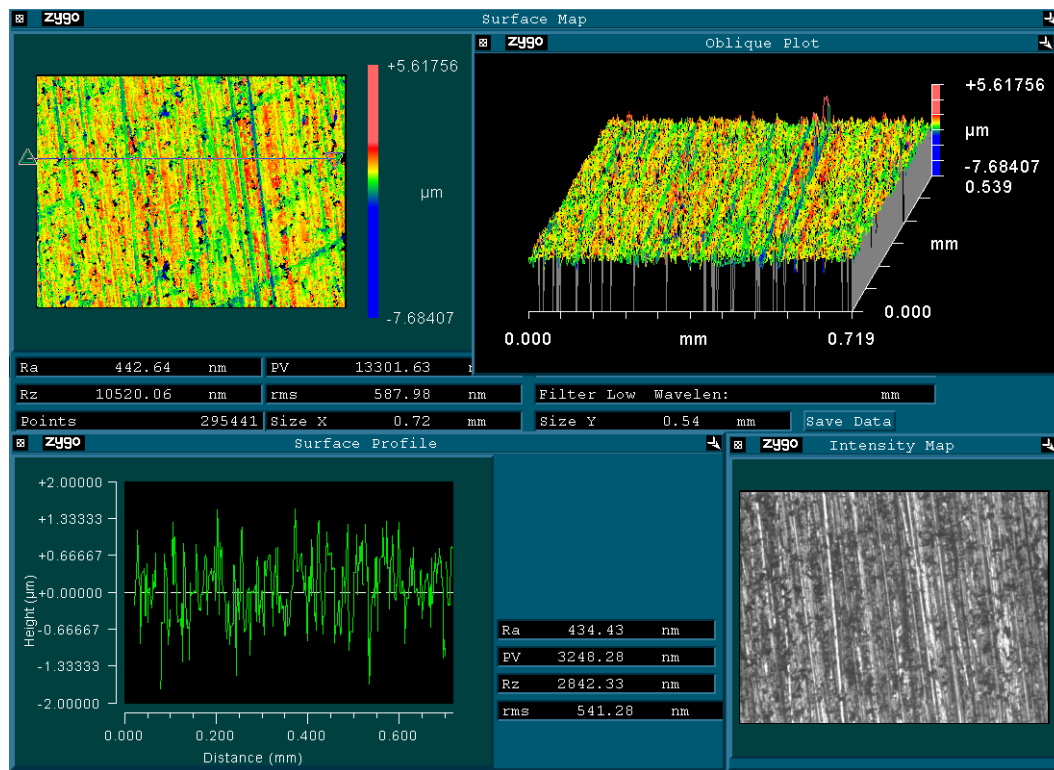


Figure 3.7 The profile of the boiling surface produced by emery sandpaper with average surface roughness of 470 nm.

### 3.5 High Speed Imaging of the Boiling Process:

The boiling process was captured using high speed imaging. A Photron 1024 PCI high-speed camera fitted with a TV zoom lens 18-108 mm and F/2.5 to F/16 from Navitar® was fixed on a tripod to capture the boiling phenomenon through one of the setup side windows. The other window was used for illumination using a single 250 W halogen lamp. A photograph of the setup is provided in Fig. 3.8. High speed images were captured in greyscale at 3000 frames per second and a resolution of 512 x 512. For the magnification purpose, the imaging spatial resolution was approximately 39 pixels per mm (1000 pixels per in).



Figure 3.8 the experimental setup with the high speed imaging .



### 3.6 Determination of Heat Flux ( $q''$ ) and Surface Temperature ( $T_s$ )

In order to determine the heater surface temperature and the heat flux through the surface, the temperature distribution of the copper block need to be established. Therefore, three thermocouples at axial distances 6.5, 14.3 and 22.15 mm from the surface of the copper block were installed at the radial centre of the copper block. To determine the heat flux  $q''$  and the surface temperature  $T_s$ , it is assumed that the heat loss in radial direction in copper block is negligible so that the temperature distribution in the copper block is linear and takes the form:

$$T = aX + b \quad (3.5)$$

Where

$$a = \frac{n \sum x_i T_i - \sum x_i \sum T_i}{n \sum x_i^2 - \sum x_i^2} \quad (3.6)$$

And

$$b = \frac{\sum T_i \sum x_i^2 - \sum T_i x_i \sum x_i}{n \sum x_i^2 - (\sum x_i)^2} \quad (3.7)$$

In which ;  $n$  is the number of the reading ,  $i$  is the reading .

The surface temperature can be calculated at  $X=0$  using the recorded temperature.

Therefore, using (3.5)

$$T_s = b \quad (3.8)$$

or

$$T_s = \frac{\sum T_i \sum x_i^2 - \sum T_i x_i \sum x_i}{n \sum x_i^2 - (\sum x_i)^2} \quad (3.9)$$

To calculate the heat flux from the experimental measurements , using the conduction equation for 1D

$$q'' = k dT/dx \quad (3.10)$$

To find  $dT/dx$  , combine equations (3.6) , (3.7) with (3.5) and differentiate the resultant equation with respect with  $x$  to get :

$$q'' = k \frac{n \sum x_i T_i - \sum x_i \sum T_i}{n \sum x_i^2 - (\sum x_i)^2} \quad (3.11)$$

In each scanned temperatures , equations (3.9) and (3.11) have been used to calculate the surface temperature and the heat flux respectively .

The thermocouples were used in this study were calibrated against RTD has error of  $\pm 0.025$  °C. Therefore,  $\pm 0.025$  °C was considered as the error limit in the thermocouples. The embedded thermocouples were 1.0 mm in diameter, and the drilled holes in the copper block were 1.1 mm diameter. Therefore, the limits of the error in the thermocouple location were  $\pm 0.05$  mm. The locations of the thermocouples are represented in Fig. 3.2. Examples of the calculated temperature distributions with error bars are shown in Fig 3.9.

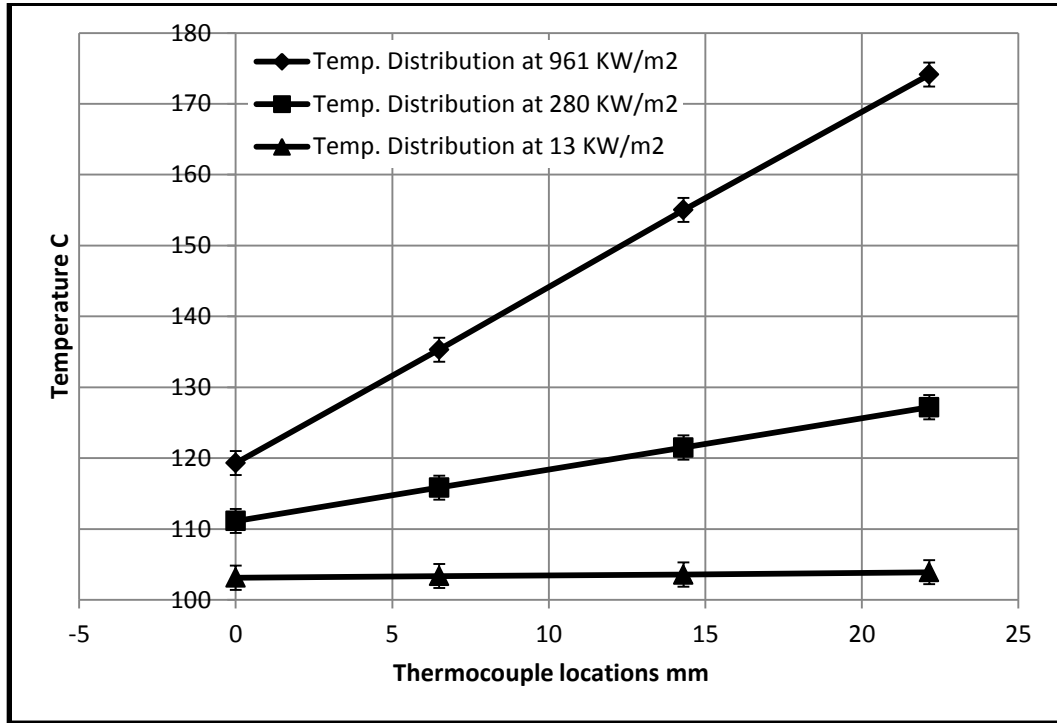


Figure 3.9 Measured temperature distributions at different heat flux inputs.

### 3.7 Uncertainty Analysis

The error propagation for any calculated value that depends on experimental measurements association with their error can be calculated by Eq. (3.3) [26] as follow :

$$w_R = \left[ \left( \frac{\partial R}{\partial x_1} w_1 \right)^2 + \left( \frac{\partial R}{\partial x_2} w_2 \right)^2 + \dots + \left( \frac{\partial R}{\partial x_n} w_n \right)^2 \right]^{1/2} \quad (3.12)$$

Where,  $w_R$  is the uncertainty in  $R$ ,  $R$  is any calculated parameter, and  $x_n$  is the parameters that  $R$  depends on, and  $w_n$  is the uncertainty in the independent parameters.

### 3.7.1 Uncertainty in Calculating the Surface Temperature ( $T_s$ )

To calculate the surface temperature, three thermocouples axially embedded in the copper block as shown in Fig.3.2 . The uncertainty is then calculated using Eq.(3.9) and Eq. (3.12), which yields an uncertainty of  $\pm 0.18$  °C. Considering an average surface temperature of 110 °C, the uncertainty in the calculated surface temperatures is about 0.16 %.

### 3.7.2 Uncertainty in the Calculation of the Surface Heat Flux ( $q''$ )

The uncertainty in the calculated heat flux is due to the uncertainty in the temperature profile in the copper block. Calculating the uncertainty in  $q''$  using Eq. (3.11) and Eq. (3.12) gives a maximum experimental uncertainty of  $\pm 4.5$  kW/m<sup>2</sup>. For an average heat flux of 500 kW/m<sup>2</sup>, this gives an uncertainty of about 0.9 %.

### 3.7.3 Uncertainty in Bulk Fluid Liquid Saturation Temperature $T_{sat}$

The bulk fluid temperature was measured using two thermocouples. The saturation temperature was then calculated using the average of the two reading using Eq. (3.13) :

$$T_{sat} = \frac{T_1 + T_2}{2} \quad (3.13)$$

The error in each thermocouple was  $\pm 0.025$  °C as they were calibrated against RTD has this accuracy. A combined error of  $\pm 0.02$  °C in the liquid saturation temperature. For an average liquid saturation temperature of 100 °C, the uncertainty in the calculated bulk fluid temperature is about 0.02 %.

### 3.7.4 Uncertainty in the Calculated Surface Superheat ( $T_s - T_{sat}$ )

The uncertainty in the surface superheat is due to the uncertainty in surface temperature and liquid saturation temperature. Using Equation (3.12), the maximum uncertainty in surface superheat is  $\pm 0.181$  °C.

### 3.7.5 Uncertainty in Heat Transfer Coefficient ( $HTC$ )

Heat transfer Coefficient ( $h$ ) was calculated using Newton's law of cooling, which takes the form:

$$q'' = h (T_s - T_{sat}) \quad (3.14)$$

Therefore, combining Eq.(3.12) and Eq.(3.14) leads a maximum error of  $\pm 0.394$  kW/m<sup>2</sup>C. Summary for the calculated uncertainties in table 3.1.

**Table 3.1 Summary for the calculated uncertainties.**

Calculated Quantity	Mathematical Formula	Uncertainty
Surface Temperature ( $T_s$ )	$T_s = \frac{\sum T_i \sum x_i^2 - \sum T_i x_i \sum x_i}{n \sum x_i^2 - (\sum x_i)^2}$	$\pm 0.18$ °C
Surface Heat Flux ( $q''$ )	$q'' = k \frac{n \sum x_i T_i - \sum x_i \sum T_i}{n \sum x_i^2 - (\sum x_i)^2}$	$\pm 4.5$ kW/m <sup>2</sup>
Bulk Fluid Saturation Temperature $T_{sat}$	$T_{sat} = \frac{T_1 + T_2}{2}$	$\pm 0.02$ °C
Surface Superheat ( $T_s - T_{sat}$ )	$T_s - T_{sat}$	$\pm 0.181$ °C.
Heat Transfer Coefficient ( $HTC$ )	$q'' = h (T_s - T_{sat})$	$\pm 0.394$ kW/m <sup>2</sup> C

### 3.8 Nanofluids Preparation

It is reported in the literature that Alumina oxide ( $Al_2O_3$ ) was used by most of the researchers. Therefore, it is used in this study. The initial particles size before mixing with the base fluid was 10 nm, as provided by the manufacturer. Distilled water was used as the based fluid for the prepared nanofluids. In order to enhance the stability of the prepared nanofluids, a surfactant, Sodium dodecylbenzenesulfonate (SDBS) was used. Wang et. al. [27] performed an investigation of the effect of surfactants on the stability of nanofluids. They determined the optimum conditions to have stable nanofluid suspensions. They reported that a 0.1% weight fraction of SDBS provided good stability of alumina-water based nanofluids of 0.05% by weight. Therefore, SDBS has been used in this study. The desired mass of the SDBS was measured carefully and mixed with five (5) liter of distilled water. Then, the  $Al_2O_3$  nanoparticles of 0.05% by weight was added to the solution and placed in an ultrasonic path. The sonication time was chosen to be 30 minutes as was recommended by Yousefi et. al. [28]. It should be noted that surfactants have shown an influence on the heat transfer performance [29, 30]. Therefore, another nanofluids suspension was prepared without SDBS in order to assess the effect of SDBS on the stability and heat transfer of the suspensions.

A Zetasizer Nano ZS by Malvern® has been used to measure the actual particles' size of the solution using dynamic light scattering (DLS). This technique measures the diffusion of particles moving under Brownian motion (the random motion of the particles) in which a laser beam shines through the suspension. A special light detector measures the scattered light for a period of time and a mathematical analysis is performed to correlate the light fluctuation. Finally, the data is processed to identify the particles size and the number of particles in each size range.

A sample of the DLS measurements of the nanofluids and the nanosuspensions (i.e., nanofluids plus SDBS) used in this study is shown in Fig. 3.10. It can be seen that in the presence of the surfactant, nanosuspensions, the dominant particle size did not change

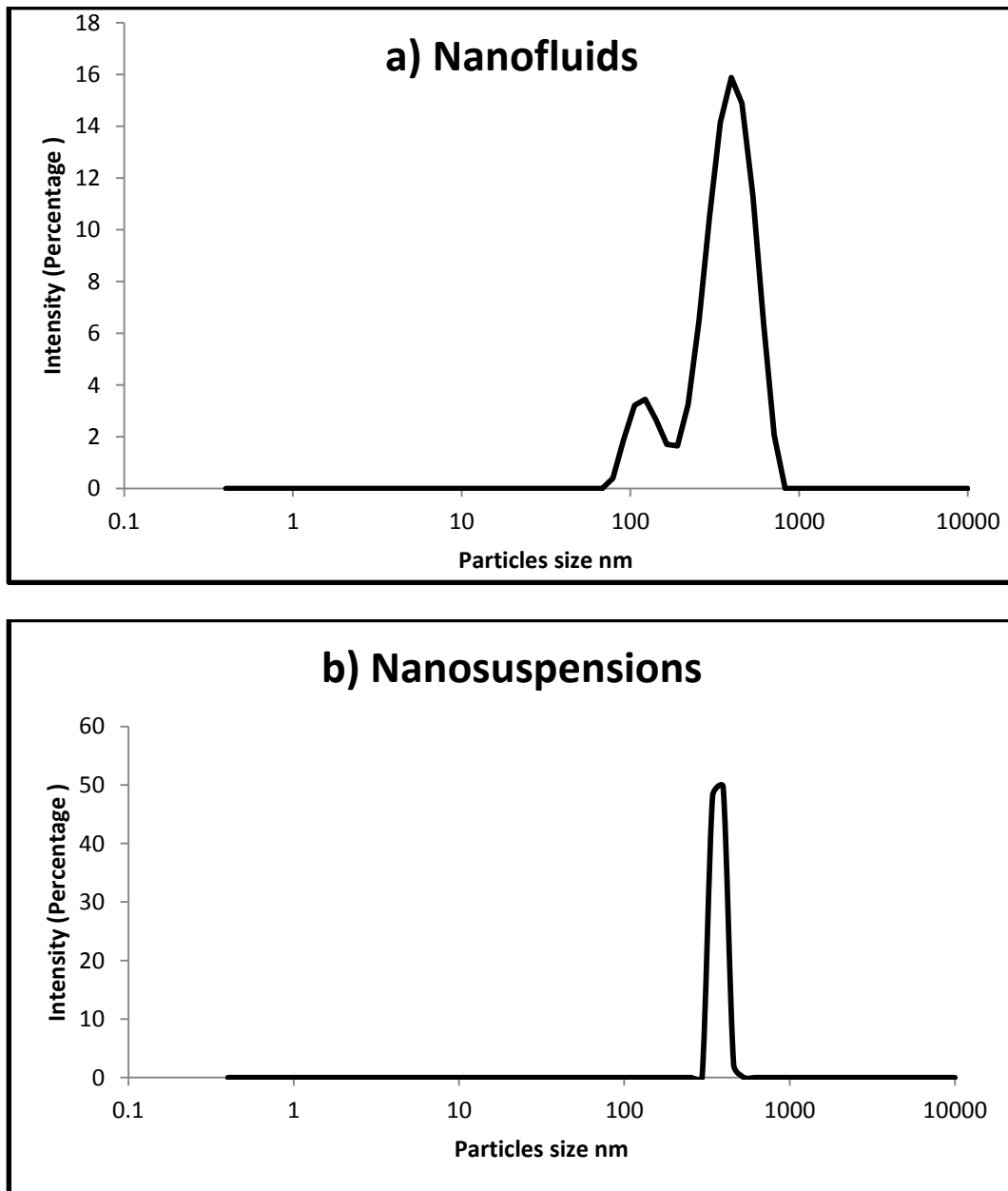


Figure 3.10 Actual particles' size using DLS: a) Nanofluids. B) Nanosuspensions .

significantly. However, the distribution was a bit better than in the case of nanofluids where two different peaks were observed. The large peak had an average particle size of  $405.9 \pm 118$  nm, with intensity of 85.3%. The second peak had an average particle size of  $129.4 \pm 31$  nm with intensity of 14.7%. The DLS measurements for the nanosuspensions had only one peak at  $371.4 \pm 58$  nm. These results show that the surfactant enhanced the agglomerated particle size distribution.

### **3.9 Experiment Procedures**

Before each experiment, the boiling vessel was washed out thoroughly using distilled water in order to remove any dust or residual of nanoparticles from the previous experiment. The setup was then reassembled and the heaters and thermocouples were reconnected. The vessel was filled with five liters of the required liquid, i.e., distilled water, nanofluids, or nanosuspensions, based on the intended experiment. The bulk liquid heater and the air heater were switched on and set at the automatic mode to heat up the liquid and the air around the copper block to about  $104^{\circ}\text{C}$  and  $110^{\circ}\text{C}$ , respectively. The controller was set to slightly higher temperatures to minimize any heat loss that might occur. Once the temperature of the liquid reached the saturation temperature, the bulk liquid heater was switched to the manual mode and set at 50% of its full input power. The inlet valve of the condensing water was opened at a flow rate of about  $300 \text{ cm}^3/\text{min}$ . The heater of the condensing water was switched on to control the condensing water temperature to about  $49^{\circ}\text{C}$ . These conditions were found appropriate to maintain the liquid temperature at saturation and prevent any bulk liquid sub-cooling. The main heater was switched on and set at the manual mode at about 2% of its power input for about 15 minutes in order to remove any non-condensable gases within the liquid. After 15 minutes, the main heater was set at 1% of its power until the copper block reached



steady-state and the first reading of the three temperatures within the copper block were recorded. It should be noted here that the steady-state condition was assumed when the change in the readings of the temperatures of the copper block were within  $0.1^{\circ}\text{C}$  for a period of 30 seconds. The power input to the main heater was incrementally increased and the same procedure was repeated.

After the experiment was completed, all heaters were switched off and the liquid was allowed to cool down using the sub-cooling coil. The liquid was then drained out of the vessel and the boiling surface was taken out for inspection.

### **3.10 Parameters Investigated and Experimental Conditions**

As indicated before, three surfaces have been prepared and used to carry out pool boiling experiments. The details of these surfaces are as follows:-

#### **1) Ultra Smooth Machined Surface of $R_a = 6 \text{ nm}$ (Surface 1)**

A number of pool boiling experiments has been performed on a very smooth and consistent boiling surface prepared using an ultra-precision diamond turning. The average surface roughness for the smooth boiling surface was maintained at  $6 \pm 3 \text{ nm}$  for all experiments. The aim of this stage is to investigate nanofluids pool boiling using nanoparticles with an average size of the same order of magnitude as of the average surface roughness of the heater surface. It is worth noting here that a new machined surface was used for each boiling experiment.

#### **2) Rough Machined Surface of $R_a = 470 \text{ nm}$ (Surface 2)**

A rough surface has been prepared by using a conventional lathe machine. The average surface roughness was kept at  $470 \pm 30 \text{ nm}$ .

**3) Rough Polished Surface of  $R_a = 470$  nm (Surface 3)**

A third surface was polished by using emery sandpaper to produce the same  $R_a$  obtained for surface 2, which was machined using a conventional lathe machine.

The set of experiments performed on the three prepared surfaces is provided in table 3.1. The nanoparticles concentration was kept at 0.05% by weight for all experiments. The SDBS was added at a concentration of 0.1% by mass. The range of the surface temperature was up to 120<sup>0</sup> C while the maximum heat flux was up to 1050 kW/m<sup>2</sup>.

**Table 3.2 Details of the experiments performed using the three prepared surfaces**

<b>Surface Preparation Method</b>	<b>Fluid Type</b>	<b>Initial Surface Condition</b>	<b>Average Surface Roughness</b>
<b>Diamond turning machine</b>	Distilled water	Clean surface	6±3 nm
	Distilled water and SDBS only	Clean surface	6±3 nm
	Nanosuspensions	Clean surface	6±3 nm
	Distilled water	Nanoparticles' suspension deposited surface	NA
	Nanofluids	Clean surface	6±3 nm
	Distilled water	Nanofluids deposited surface	NA
<b>Conventional lathe machine</b>	Distilled water	Clean surface	470±30 nm
	Distilled water and SDBS only	Clean surface	470±30 nm
	Nanosuspensions	Clean surface	470±30 nm
	Distilled water	Nanoparticles' suspension deposited surface	NA
	Nanofluids	Clean surface	470±30 nm
	Distilled water	Nanofluids deposited surface	NA
<b>Emery sandpaper</b>	Distilled water	Clean surface	470±30 nm
	Distilled water and SDBS only	Clean surface	470±30 nm
	Nanosuspensions	Clean surface	470±30 nm
	Distilled water	Nanoparticles' suspension deposited surface	NA
	Nanofluids	Clean surface	470±30 nm
	Distilled water	Nanofluids deposited surface	NA

## Chapter 4 Results and Discussion

In this chapter, the validity of the experimental setup is presented in section 4.1. The repeatability of the experiments is addressed in section 4.2. The experimental results obtained for the three surfaces are presented and discussed in section 4.3. The effect of the surface preparation method and the effect of the transient nature of the nanoparticles deposition are presented in sections 4.4 and 4.5, respectively.

### 4.1 Validation of the Experimental Setup

In order to validate the experimental setup, the boiling curve obtained for distilled water using surface 1 (ultra-smoothed machined with  $R_a = 6$  nm) was obtained and compared with Rohsenow's pool boiling correlation [31] given by equation (4.1)

$$\frac{C_p \cdot \Delta T}{h_{fg}} = C_{sf} \left[ \frac{q''}{\mu \cdot h_{fg}} \sqrt{\frac{\sigma}{g(\rho - \rho_g)}} \right]^m \left( \frac{C_p \cdot \mu}{k} \right)^n \quad (4.1)$$

Rohsenow suggested  $m=1/3$ ,  $n=1$ , and  $C_{sf}=0.0128$  for the case of pool boiling of water on a copper boiling surface. However, since the value of  $C_{sf}$  mainly depends on the fluid-surface combination and can be determined experimentally, the current data were found to fit well with  $C_{sf}=0.0105$ . The current experimental data and values obtained from Rohsenow's correlation are plotted in Fig.4.1. One can easily note that Rohsenow's correlation is in good agreement with the current experimental data.

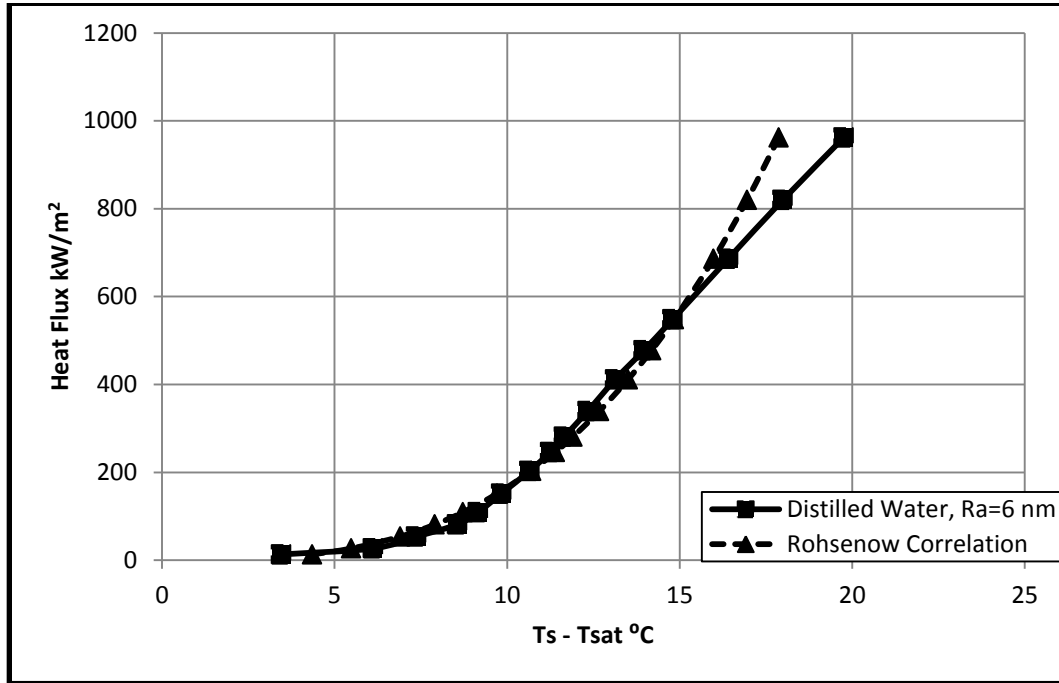


Figure 4.1 Comparison between experimental data of boiling distilled water on surface 1 and data obtained using Rohsenow’s correlation.

#### 4.2 Repeatability Test

In order to verify the consistency of the ultra-smooth surface (surface 1) and the repeatability of the current experiments, three fresh surfaces have been used during three distilled water and three nanosuspensions boiling experiments. Results of these experiments are as shown in Figures 4.2 and 4.3, respectively.

It should be noted that all surfaces were clean and fresh and have been used only once for each experiment. One can clearly see from Fig. 4.2 that almost identical water boiling curves were produced. However, the data obtained for the nanosuspensions, Fig. 4.3 has a maximum surface temperature deviation of less than 1.5 °C. This might be explained as the boiling of nanosuspensions is more sensitive to any change in the experiment conditions since nanosuspensions have higher number of bubbles during the

boiling process than the distilled water. These results shows reasonable repeatability of the current experimental data.

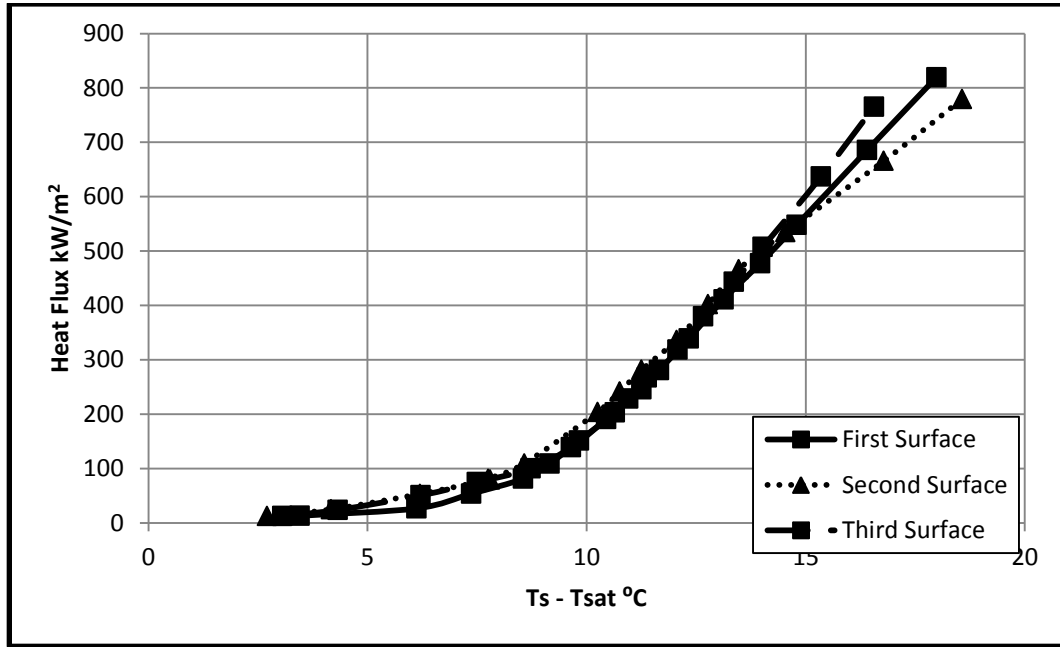


Figure 4.2 Repeatability test for distilled water boiling experiments using surface 1.

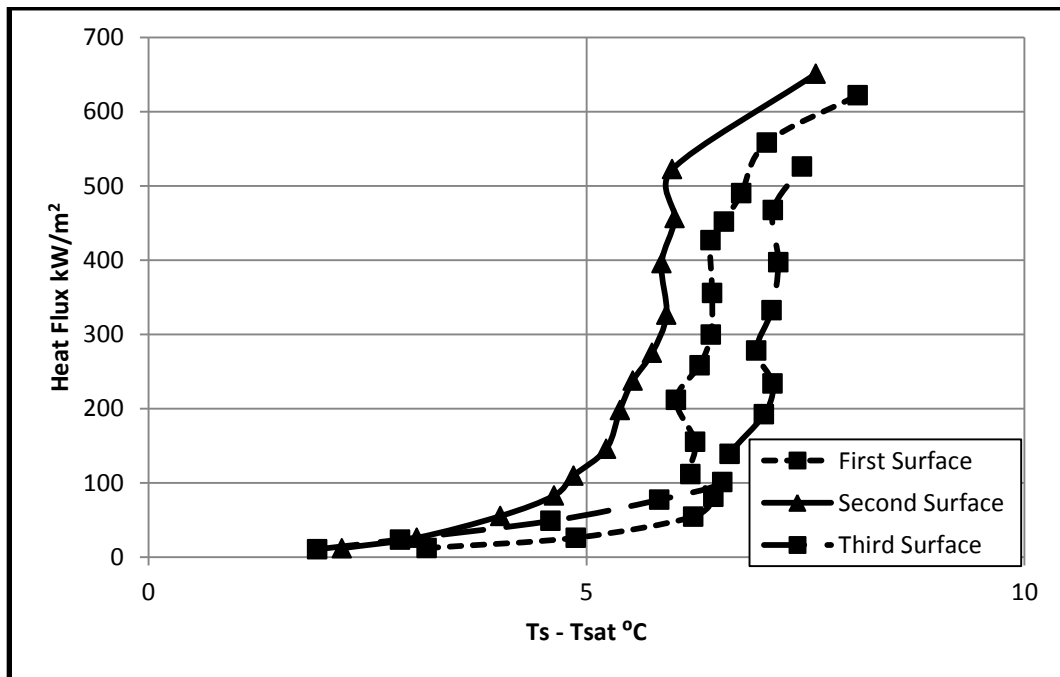


Figure 4.3 Repeatability test for nanosuspensions boiling experiments using surface 1.

### 4.3 Effect of the Boiling Fluid on the Rate of Boiling Heat Transfer

#### 4.3.1 Results Obtained using Surface 1(Ra=6 nm)

Details of the experiments performed on surface 1 that prepared by diamond turning machine are listed on Table (4.1). The pool boiling curves obtained for the boiling experiments carried out for the different liquids on the ultra-smooth surface (surface 1) are shown in Fig 4.4. The corresponding heat transfer coefficient versus heat flux is shown in Fig 4.5. The boiling phenomenon is recorded using high speed imaging is shown in Fig.4.6. One can see that at a certain heat flux, boiling of a certain fluid can give higher or lower in the temperature of the surface superheat. In other words, when the curve is shifted to the left, it is enhancement in the heat transfer. Similarly, when the boiling curve is shifted to the right, it is deterioration in the heat transfer performance.

**Table 4.1 Details of pool boiling experiments performed on surface 1 ( Ra=6 nm).**

<i>Designations</i>	<i>Fluid type</i>	<i>Onset of nucleate boiling</i>	<i>HTC @400 kW/m<sup>2</sup> (kW/m<sup>2</sup> °C)</i>	<i>HTC ratio</i>
<i>Water</i>	Distilled water	9.8	31	1
<i>NF</i>	Nanofluids	7.45	40.5	1.3
<i>Water on NFDS</i>	Distilled water on nanofluids deposited surface	9.5	32	1.03
<i>SDBS</i>	Distilled water and SDBS surfactant	6.2	47	1.51
<i>NS</i>	Nanosuspensions	6.5	62	2
<i>Water on NSDS</i>	Distilled water on nanosuspensions deposited surface	10.5	30	0.96

It can be seen that from Figures 4.5 and 4.6 that the SDBS dispersed in distilled water has the maximum enhancement with respect to the distilled water. This enhancement can be attributed to the decreased surface tension as concluded by some researchers [29, 30]. This decrease in the surface tension leads to decrease in the bubble size and increase in the number of bubbles as it can be clearly seen in the recorded images Fig.4.6. The nanofluids HTC is enhanced about 1.3 times of the HTC of the base fluid at  $400 \text{ kW/m}^2$ . The maximum enhancement is found for the nanosuspensions in which the HTC is two times of that of the distilled water at  $400 \text{ kW/m}^2$  heat flux. The boiling curves for boiling experiment of distilled water on nanofluids deposited surface (NFDS) and nanosuspensions deposited surface (NSDS) are almost identical with the boiling curve of the same liquid on clean surface. This can explain that the effect of the deposition layer in both cases ( nanofluids and nanosuspensions) is minimal and the HTC enhancement is due the change in the thermo-physical properties. It is worth noting here that the CHF has increased significantly in the case of nanofluids due to the enhanced surface wettability, which is in agreement with observations reported in the literature [20].

The observed enhancement in HTC could be attributed to the higher thermal conductivity of nanofluids. Mikic and Rohsenow [32] discussed the basic mechanism of the boiling process for pure liquids. As a bubble departs from the boiling surface, the bubble removes with it a certain amount of superheated liquid layer and pump it away from the surface. Following that, an amount of liquid at a temperature of  $T_{sat}$  flows to the heated surface and comes in contact with the heated surface. Then, the surface heat flux is given by:



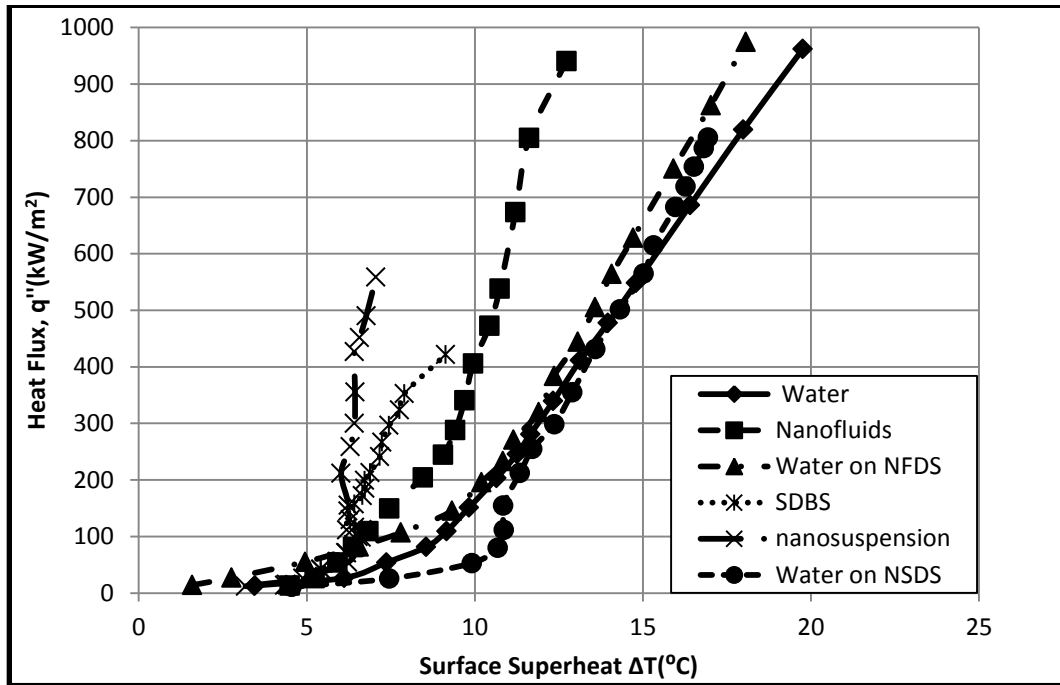


Figure 4.4 Pool boiling curves obtained from boiling experiments performed using surface 1.

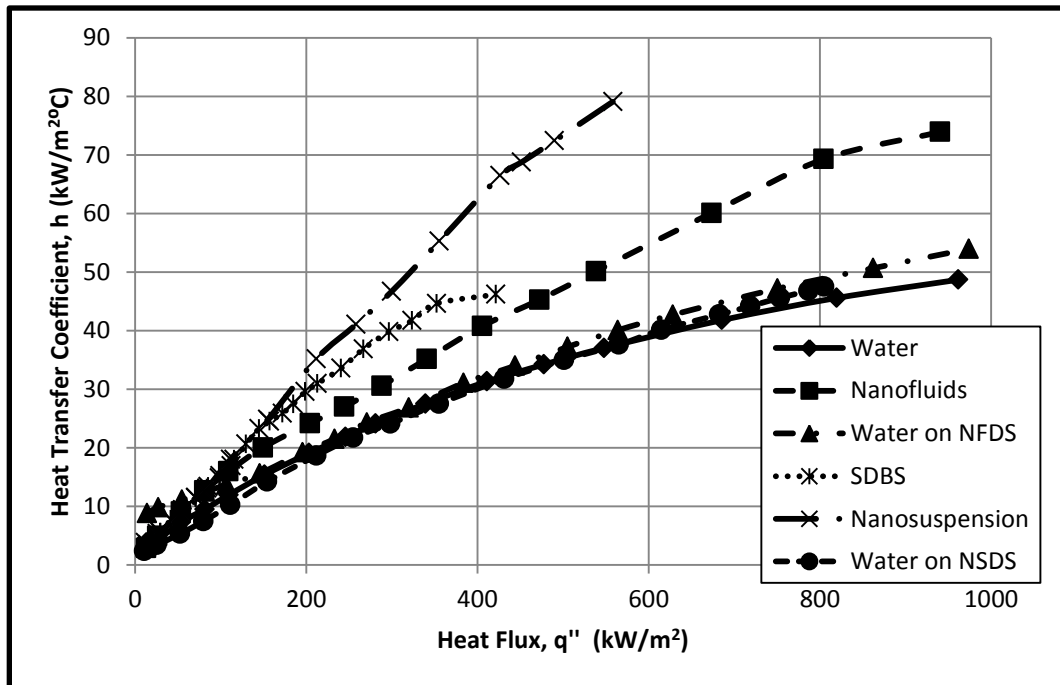


Figure 4.5 Heat transfer coefficient for different fluids using surface 1.

$$\frac{q}{A} = \frac{k\Delta T}{\sqrt{\pi\alpha t}} \quad (4.1)$$

Where ;  $q$  is the heat flux,  $A$  area of the boiling surface,  $k$  thermal conductivity of the liquid,  $\Delta T$  is degree of superheat,  $\pi$  is 3.14 ,  $\alpha$  thermal emissivity , and  $t$  is time.

A similar process exists in the case of nanofluids, except that the thermal conductivity of the superheated layer is associated with the change in the nanoparticles concentration in that layer. Taking into account the deposition mechanism that discussed by Kim et. al. [20] and Kwark et. al. [21] in which the microlayer evaporation is responsible for the nanoparticles deposition, as the number of active nucleation sites increases, the nanoparticles concentration increases in the superheated layer and therefore ; the thermal conductivity in the superheated layer increases, regardless of the thermal conductivity of the bulk liquid.

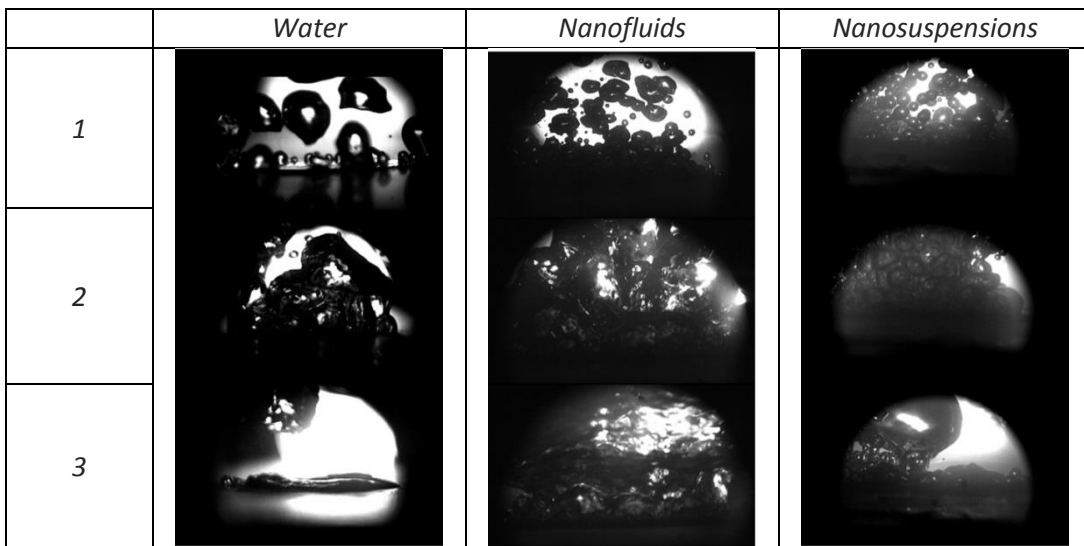


Figure 4.6 Images recorded during boiling experiments using surface 1, the heat flux for : Water: 1) 53.87 kW/m<sup>2</sup>, 2) 411.3 kW/m<sup>2</sup>, 3) 1126 kW/m<sup>2</sup> (CHF), Nanofluids: 1) 81.22 Kw/m<sup>2</sup>, 2) 405.5 kw/m<sup>2</sup>, 3) 940.6 kW/m<sup>2</sup>, Nanosuspensions: 1) 54.2 kW/m<sup>2</sup>, 2) 426.6 kW/m<sup>2</sup>, 3) 640 kW/m<sup>2</sup>(CHF).

This could explain how low concentration nanofluids could still enhance the heat transfer, even though the measured thermal conductivity shows no difference with respect to the thermal conductivity of the base fluid [21].

Fig.4.6 Shows that the bubble size in the case of distilled water and nanofluids are almost the same which confirms that the effect of low nanoparticles concentration to change surface tension of the liquid is minimal [33] . On the other hand, the presence of SDBS surfactant decreases the surface tension and therefore decreases the bubble size compare to the pure liquid.

#### **4.3.2 Results Obtained using Surface 2 (Ra=470 nm)**

Details of the experiments performed on surface 2 that prepared by conventional lathe machine are listed on Table (4.2). The pool boiling curves and HTC versus heat flux obtained using surface 2 are shown in Figs. 4.7 and 4.8. The boiling phenomenon is recorded using high speed imaging is shown in Fig.4.9.

One can see from Figs. 4.8 and 4.9 that the boiling of the SDBS dispersed in distilled water has the greatest enhancement in the heat transfer . The HTC is calculated at  $400 \text{ kW/m}^2$  and is found to be 1.8 times of that in the case of the base fluid. This enhancement is attributed to the decrease of the surface tension that was resultant of adding the surfactant as discussed before. Also, the nanofluids experiments shown enhancement in the HTC about 1.37 of the HTC of the distilled water. Boiling of nanosuspensions shows an HTC of  $54 \text{ kW/m}^2\text{C}$  which is 1.4 times the HTC of the distilled water on clean surface.

**Table 4.2 Details of pool boiling experiments performed on surface 2 (Ra = 470 nm).**

<i>Designations</i>	<i>Fluid type</i>	<i>Onset of nucleate boiling</i>	<i>HTC @400 kW/m<sup>2</sup> (kW/m<sup>2</sup> °C)</i>	<i>HTC ratio</i>
<i>Water</i>	Distilled water	9.02	32	1
<i>NF</i>	Nanofluids	6.1	44	1.37
<i>Water on NFDS</i>	Distilled water on nanofluids deposited surface	8.3	34	1.06
<i>SDBS</i>	Distilled water and SDBS surfactant	7.4	58	1.8
<i>NS</i>	Nanosuspensions	5.6	54	1.68
<i>Water on NSDS</i>	Distilled water on nanosuspensions deposited surface	8.5	34	1.06

Experimental data have been obtained by performing boiling experiments on nanoparticles deposited surfaces show no significant effect in the heat transfer performance. Rather, they showed a delay in the onset of the nucleate boiling for both cases, as shown in Table.4.2. Therefore, the change that occurred in the surface due to nanoparticles deposition had a minimum effect and the thermo-physical properties of the nanofluids and the nanosuspensions are responsible for the heat transfer improvement.

The similar observations were reported by Narayan [9] in which pool boiling of nanofluids experiment performed on a rough surface could have enhancement in the heat transfer with respect to the base fluid. Also, the onset of nucleate boiling has been changed for each case as shown in Table 4.2.

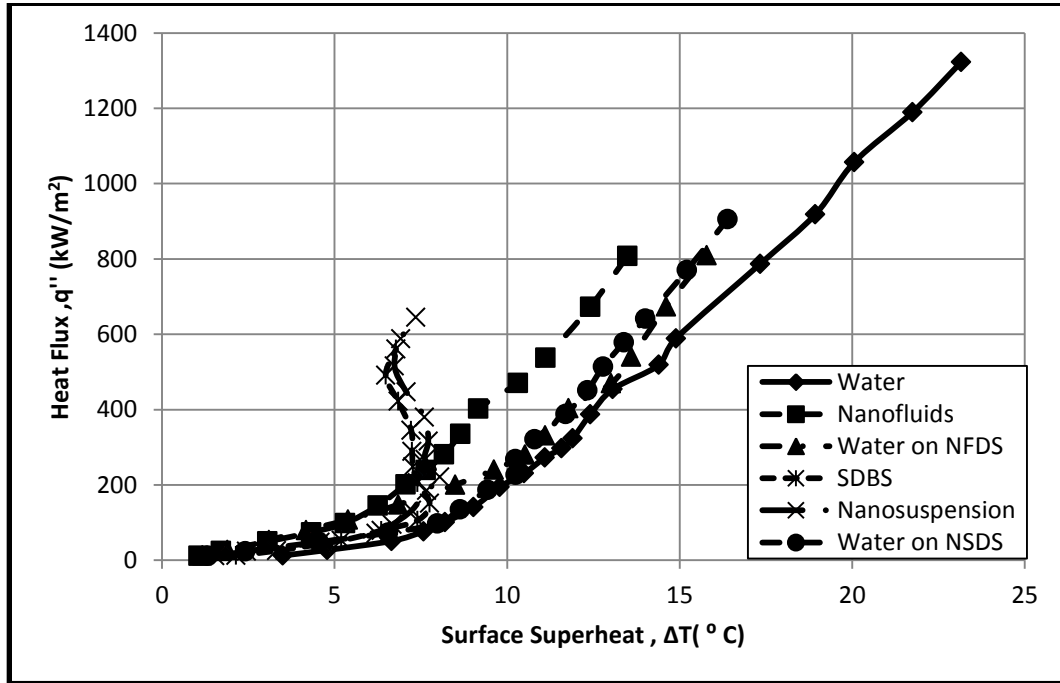


Figure 4.7 Pool boiling curves obtained from boiling experiments performed using surface 2.

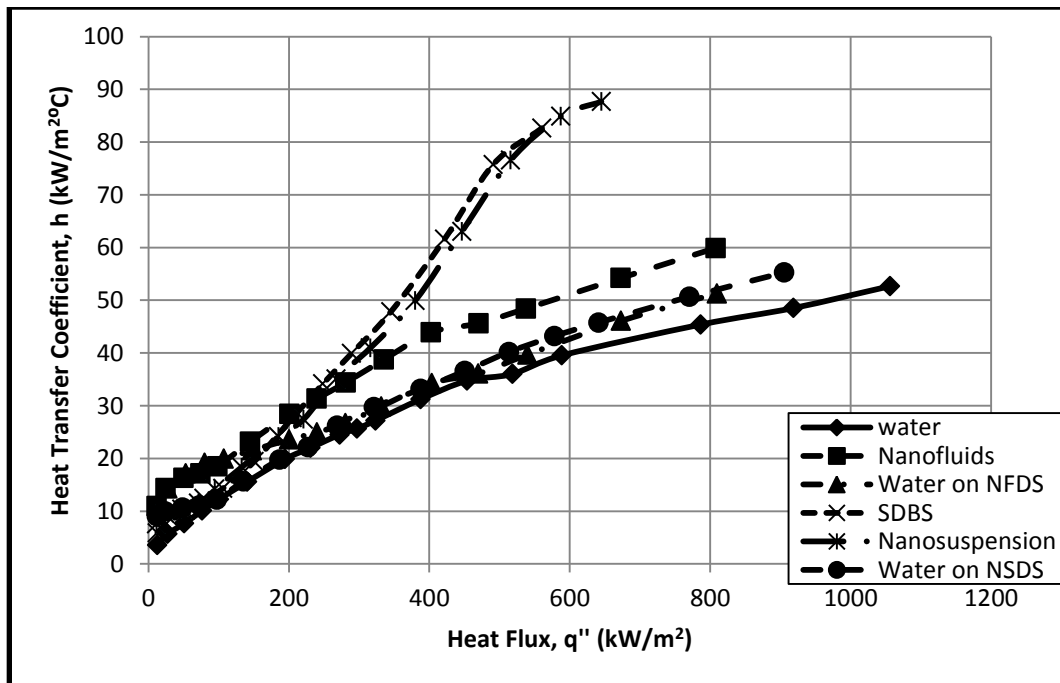


Figure 4.8 Heat transfer coefficient for boiling experiments of different fluids on surface 2.

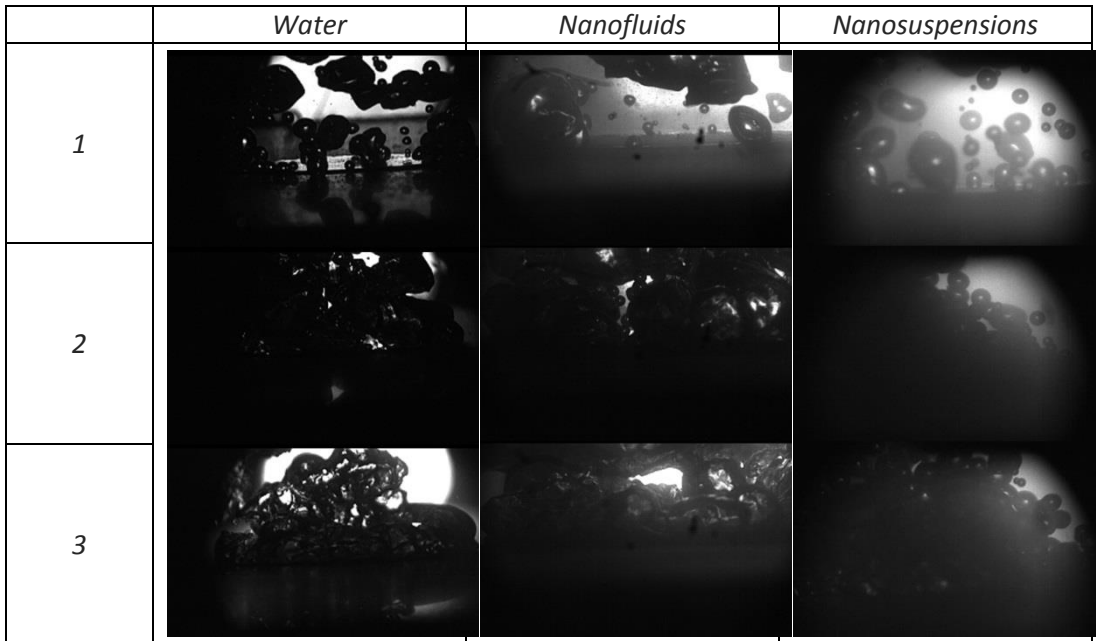


Figure 4.9 Images recorded during boiling experiments using surface 2. the heat flux for : Water: 1) 51 kW/m<sup>2</sup>,2) 272.2 kW/m<sup>2</sup>, 3) 1322 kW/m<sup>2</sup>, Nanofluids: 1) 74.1 Kw/m<sup>2</sup>, 2) 280.8 kw/m<sup>2</sup>, 3) 807.8 kW/m<sup>2</sup>, Nanosuspensions: 1) 47.5 kW/m<sup>2</sup>, 2) 220.9 kW/m<sup>2</sup>,3) 645 kW/m<sup>2</sup>.

Fig.4.9 shows that the bubble size in the nanofluids case is almost the same as it is in the distilled water. This also confirms that adding low concentration of nanoparticles does not change the surface tension of the base fluid as discussed before in 4.3.1. However, the bubble size was decrease in the case of the nanosuspensions as a result of the SDBS surfactant that causes a decrease in the surface tension.

#### 4.4.3 Results Obtained using Surface 3 (Ra=470 nm)

Details of the experimental data obtained on surface 3 that prepared by emery sandpaper is represented and discussed in this section. The boiling curves are shown in Fig.4.10. HTC versus heat flux are presented in Fig.4.11. The boiling phenomenon is recorded using high speed imaging is shown in Fig.4.12. Compare to the base fluid, boiling of the SDBS dispersed in distilled water shows improvement in the HTC and it is

1.67 time of the HTC of distilled water on clean surface at  $400 \text{ kW/m}^2$  heat flux. Similarly, the HTC is improved to 1.16 times of the base fluid in the case of the nanofluids. On the other hand, boiling curves for the water on nanofluids and nanosuspensions deposited surfaces show some changes in the heat transfer characteristics. Therefore, the improvement that occurred in the case of nanofluids and nanosuspensions could be attributed to the change in the surface texture as well as the thermo-physical properties of the fluids .

Fig.4.12 shows that the bubble size is smaller in the case of nanosuspensions with compare to the base fluid while the nanofluids show almost the same bubble size as it is in the base fluid case. This is also attributed to the decrease in the surface tension that caused by the dispersing agency .

**Table 4.3 Details of pool boiling experiments performed on surface 3 (Ra = 470 nm).**

<i>Designations</i>	<i>Fluid type</i>	<i>Onset of nucleate boiling</i>	<i>HTC @400 kW/m<sup>2</sup> (kW/m<sup>2</sup> °C)</i>	<i>HTC ratio</i>
<i>Water</i>	Distilled water	8.5	36	1
<i>NF</i>	Nanofluids	6.2	42	1.16
<i>Water on NFDS</i>	Distilled water on nanofluids deposited surface	8.3	33	0.92
<i>SDBS</i>	SDBS surfactant	6.25	60	1.67
<i>NS</i>	Nanosuspensions	5.4	70	1.94
<i>Water on NSDS</i>	Distilled water on nanosuspensions deposited surface	6.6	39	1.08

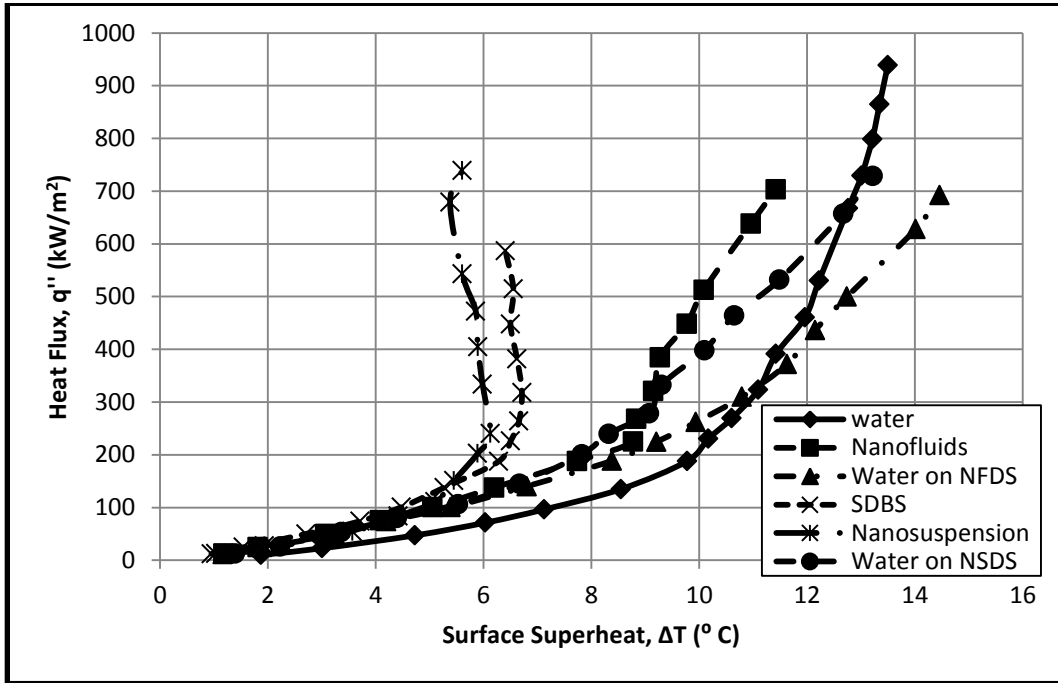


Figure 4.10 Pool boiling curves obtained from boiling experiments performed using surface 3.

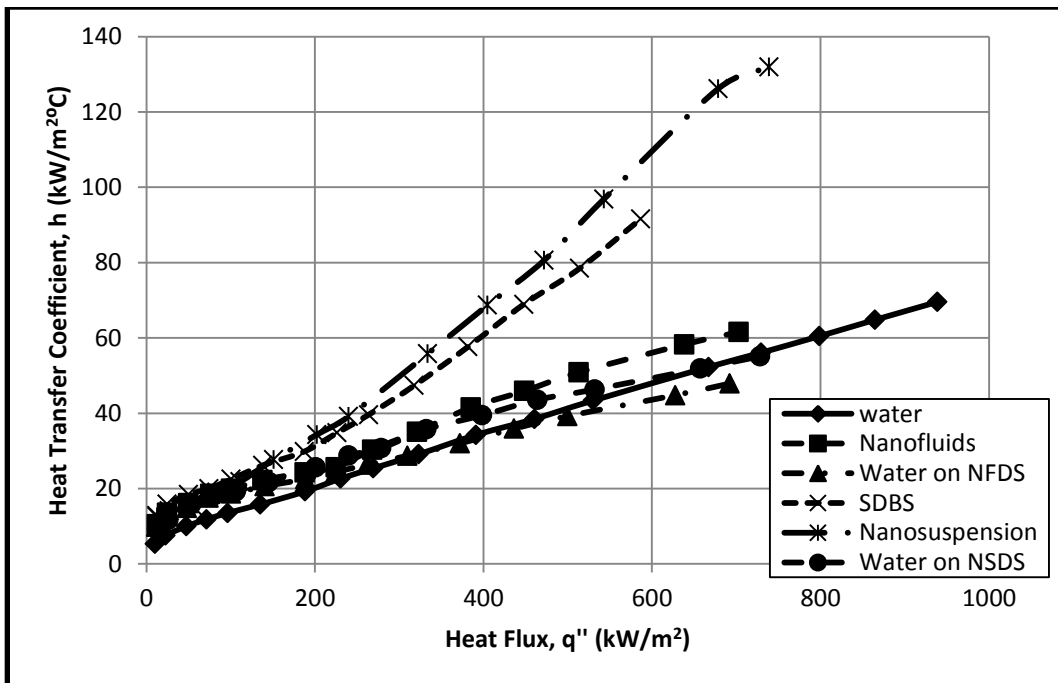


Figure 4.11 Heat transfer coefficient for boiling experiments of different fluids on surface 3.



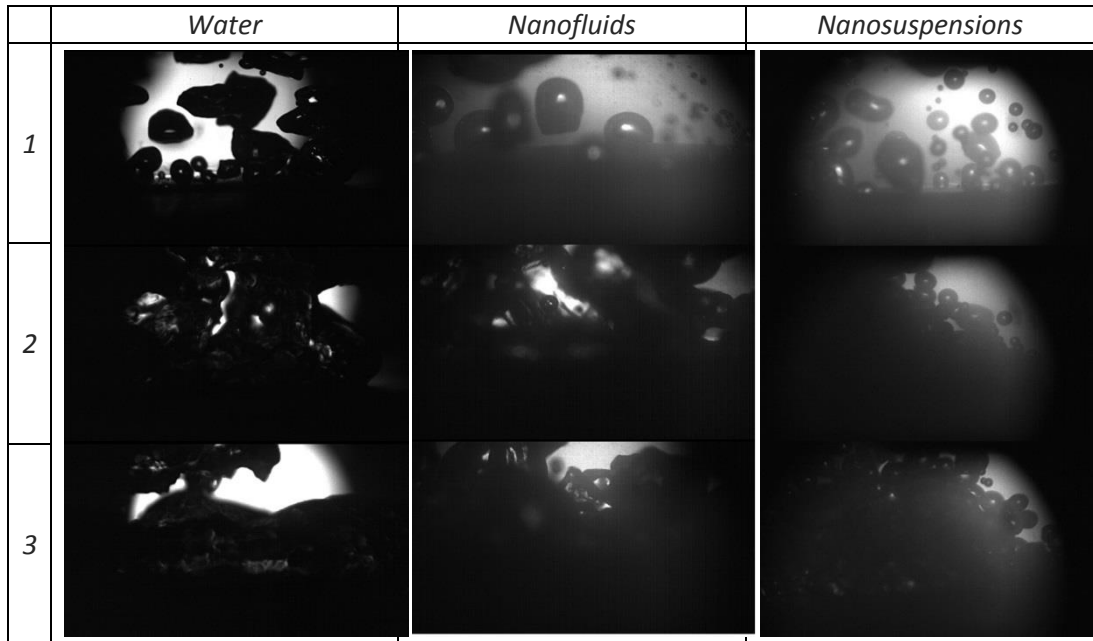










Figure 4.12 Images recorded during boiling experiments using surface 3. the heat flux for : Water: 1) 47.1 kW/m<sup>2</sup>,2) 391.1 kW/m<sup>2</sup>, 3) 938.7 kW/m<sup>2</sup>, Nanofluids: 1) 24.6 Kw/m<sup>2</sup>, 2) 267.9 kw/m<sup>2</sup>, 3) 384.9 kW/m<sup>2</sup>, Nanosuspensions: 1) 111 kW/m<sup>2</sup>, 2) 151 kW/m<sup>2</sup>,3) 739 kW/m<sup>2</sup>.

#### 4.4 The Effect of Surface Preparation Method

The effect of the surface preparation method is discussed in this section considering each type of liquid used in this study. The images for the heater surface before and after boiling experiments using the three prepared surfaces are shown in Fig.4.13.

##### 4.4.1 Effect of Surface Preparation Method Observed from Distilled water Boling Experiments

The boiling curves obtained from the boiling experiments carried out using distilled water and a clean surface using the three prepared surfaces are shown in Fig.4.14 The corresponding HTC's versus the surface heat flux are shown in Fig.4.15. Details of the surface measurements performed on the three surfaces after preparation are included in Table.4.4. Images taken for the clean surfaces are shown in Fig.4.13.

	<i>Surface 1</i>	<i>Surface 2</i>	<i>Surface 3</i>
Clean			
NFDS	NA		
NSDS			

**Figure 4.13 Images taken for the various boiling surfaces.**

Surprisingly, the boiling curves for surface 1 and 2 are almost the same, even though the two surfaces have different average surface roughness values. Moreover, the boiling curves of surfaces 2 and 3 that have the same  $R_a$  values and different preparation methods are not similar. Fig.4.15 shows the HTC for distilled water on the three surfaces

versus the heat flux. The onset of nucleate boiling for surface 1 was 9.8 °C followed by 9.02 °C for surface 2 and finally 8.5 °C for surface 3. The highest HTC was obtained for the polished surface (surface 3), while the HTCs of the other two machined surfaces (Surface 1 and 2) are almost the same. Pioro et. al. [13] pointed out that the average or the RMS value of the surface roughness do not give a good indication of the expected boiling behaviour of the surface. They indicated that for the same value of surface roughness, two extreme cases of microstructures may exist on the surface, “a plateau with peaks” and “a plateau with valleys and cavities”. Results shown in Fig 4.14 and 4.15 suggest that polishing produces surfaces having a larger number of active nucleation sites than the case of the machining methods.

**Table 4.4 Details of surface measurements performed on all three clean surfaces after preparation.**

<i>Surface number</i>	<i>Preparation Method</i>	<i>R<sub>a</sub></i> <i>(nm)</i>	<i>R<sub>z</sub></i> <i>(nm)</i>	<i>PV</i> <i>(nm)</i>	<i>RMS</i> <i>(nm)</i>
<i>Surface 1</i>	Diamond Turning Machine	5	33.6	46.25	6.33
<i>Surface 2</i>	Lathe Machine	474.47	14476.18	16832.56	627.56
<i>Surface 3</i>	Polishing	457.99	8522.46	10764.32	601.9

Moreover, the current understanding of the boiling phenomenon, stable active nucleation site can be only those micro cavities that are not filled with liquid after vapor

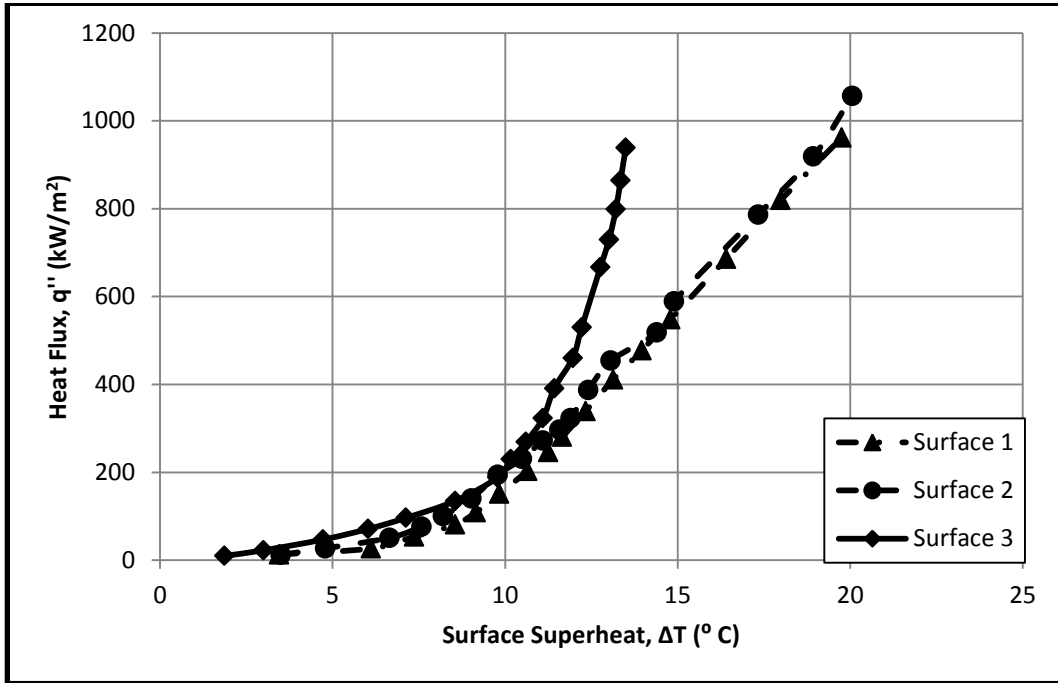


Figure 4.14 Pool boiling curves obtained for distilled water on the three clean surfaces.

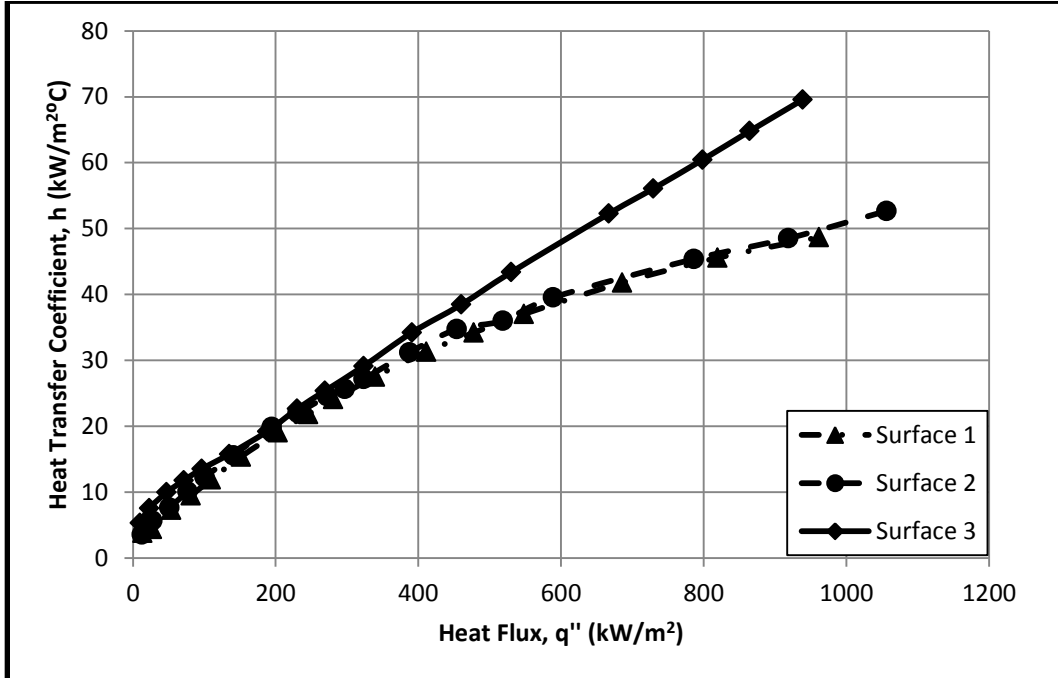


Figure 4.15 Heat transfer coefficient obtained for distilled water on the three clean surfaces.

bubble departure [13]. One might also assume that the cavities on the two machined surfaces are less capable of entrapping air as in the case of the cavities on the polished surface. These results clearly indicate that boiling heat transfer could very well depend on the method of surface preparation.

#### **4.4.2. Nanofluids**

Fig.4.16 shows the boiling curves obtained for nanofluids using the three prepared surfaces. Fig.4.17 shows the corresponding heat transfer coefficient versus the heat flux. The nanofluids resulted into an enhancement in the heat transfer in all cases as compared to the base fluid (pure water), as discussed before. The onset of nucleate boiling was at surface superheat of 7.45, 6.1, and 6.2 °C for surfaces 1, 2, and 3, respectively. One can easily note that the overall boiling curves are almost similar. The SIP that was proposed by [9] was calculated here for each surface and found to be 0.5, 47.9 and 46.4 for the three surfaces respectively. The results in the case of the polished surface are in agreement with other studies that were conducted on rough surfaces prepared by sandpaper that if the SIP far from unity, the nanofluids show enhancement [9]. However, in the case of the smooth machined surface (surface 1), the present results showing enhancement in the HTC are opposite to the results reported in [9]. As the SIP in this case is close to unity, according to [9] nanofluids should have shown a deterioration in the HTC. The current results show that the nature of the prepared surface depends on the method of preparation and hence it has a significant effect on the pool boiling results.

The surface measurements listed on Table 4.5 show that there is insignificant difference in the surface measurements before and after the nanofluids boiling

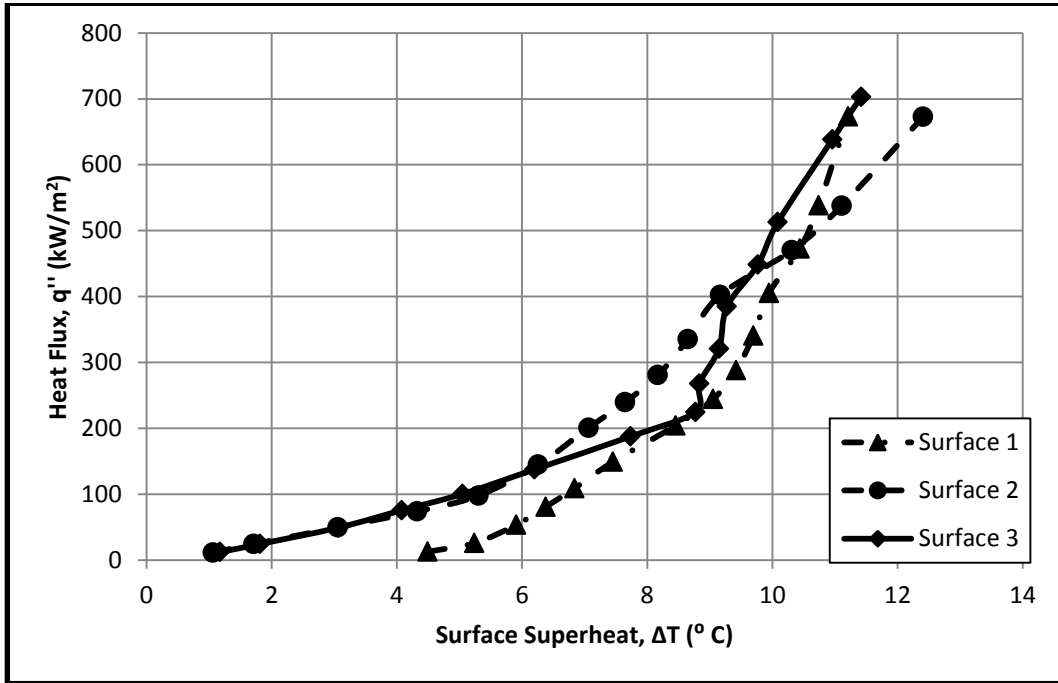


Figure 4.16 Pool boiling curves obtained for nanofluids on the three clean surfaces.

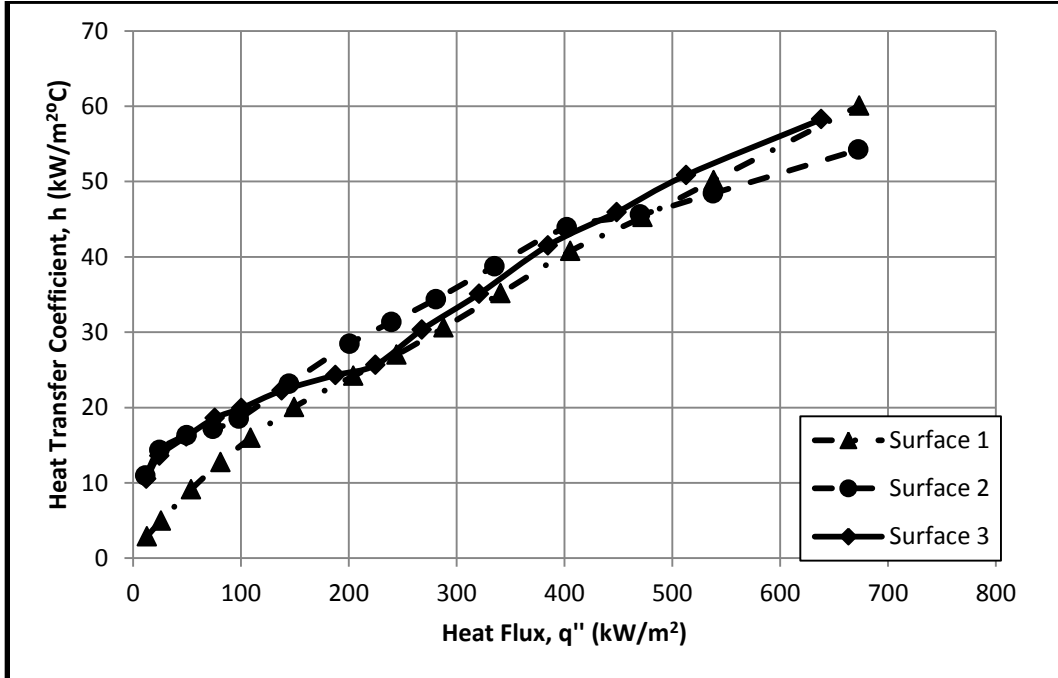


Figure 4.17 Heat transfer coefficient obtained for nanofluids on the three clean surfaces.

**Table 4.5 Results of surface measurements performed before and after nanofluids boiling experiments.**

Surface No.	Preparation method		$R_a$	$R_z$	PV	RMS	SIP
Surface 1	Diamond Turning Machine	Before	5.07	176.91	768.23	12.23	0.5
		After	NA	NA	NA	NA	
Surface 2	Lathe Machine	Before	479.88	7021.77	8373.00	600.55	47.9
		After	462.07	5534.05	6955.23	560.95	
Surface 3	Polishing	Before	464.91	11458.12	13313.55	629.99	46.4
		After	624.08	12899.39	14912.18	845.69	

experiments in the case of the machined surfaces, which suggests that nanoparticles deposition was insignificant, which could be used to explain the observed enhancement in the HTC for the three surfaces. Also, the insignificant deposition could also be used to explain that irrelevance of the SIP to these results.

#### 4.4.3 Distilled Water on Nanofluids Deposited Surfaces

In order to investigate the effect of nanoparticles deposition, boiling experiments using distilled water were performed on the nanoparticles deposited surfaces obtained after the nanofluids boiling experiments. The boiling curves of these experiments are shown in Fig.4.18. The corresponding HTCs versus the surface heat flux are shown in Fig.4.19. The HTCs of surfaces 2 and 3 are almost the same and about 50% higher than the HTC obtained for surface 1 (the ultra-smooth surface). These results are consistent with the observed level of nanoparticles deposition on the three surfaces. Surfaces 2 and 3 were almost the same, while the deposition on surface 1 was minimum as they are shown in Fig.4.13.

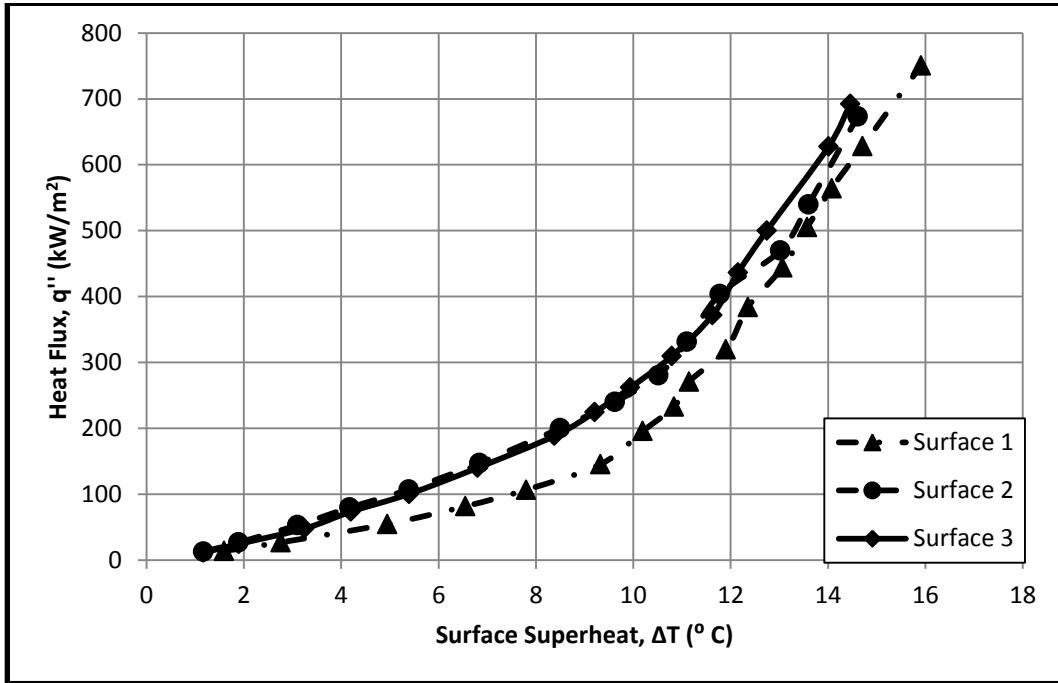


Figure 4.18 Pool boiling curves for distilled water on nanofluids deposited surfaces (NFDS) .

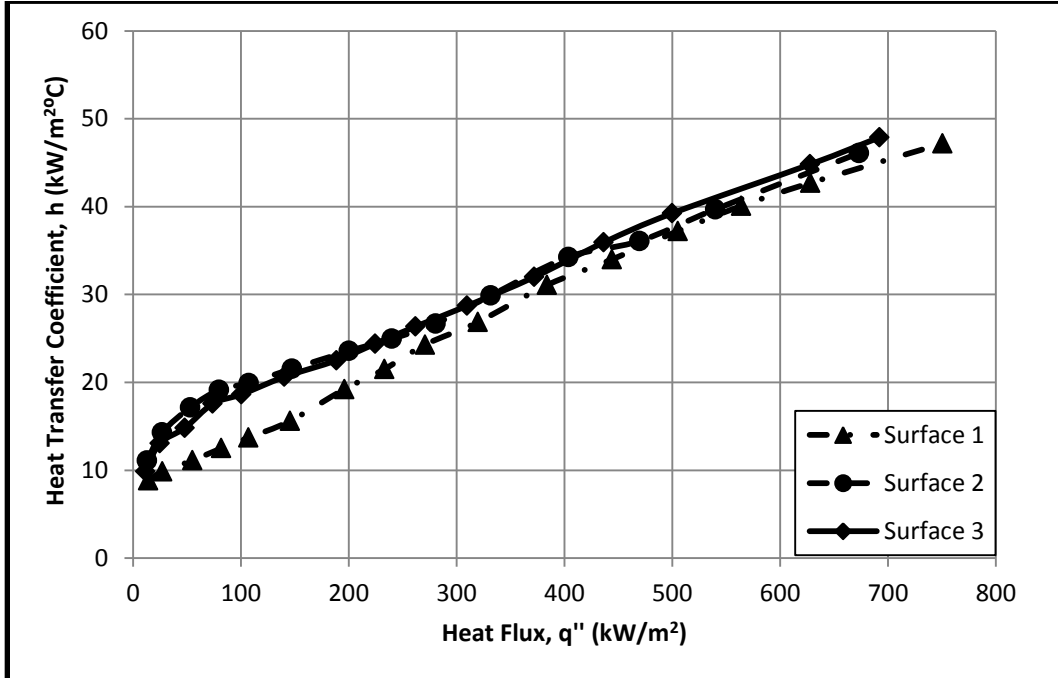


Figure 4.19 Heat transfer coefficient for distilled water on nanofluids deposited surface(NFDS).



The change in surface measurements shown in Table.4.5 suggests that this change is not always the proper tool to predict the boiling performance of nanofluids. This is because of the fact that the surface roughness measurements do not take into account the porous nature of the deposition layer. The change in the boiling performance in the of the pure base fluids in case of surface 2 and surface 3 is due to the increase in the porous nanoparticles that is concise with the number of the active nucleation sites. In other words, the more number of active nucleation sites are in the heater surface, the more amount of the nanoparticles deposition. This can clearly shows that the boiling performance is highly affected by the nature of the deposition pattern not by change in the surface roughness.

#### **4.4.4 Nanosuspensions**

Boiling curves obtained from nanosuspensions boiling experiments on the three clean surfaces are shown in Fig.4.20. The corresponding HTCs versus the surface heat flux are shown in Fig.4.21. Results of the surface measurements performed before and after the boiling experiments are shown in Table.4.6. Similar to what was mentioned before in section 4.4.2, one can easily note that the polished surface (surface 3) seems to have a larger number of active nucleation sites than the other two machined surfaces that had almost the same boiling curves. The onset of nucleate boiling was  $5.4^{\circ}\text{C}$  for surface 3,  $5.6^{\circ}\text{C}$  for surface 2, and  $6.5^{\circ}\text{C}$  for surface 1. These results signify the surface papering method which clearly affect the boiling performance.

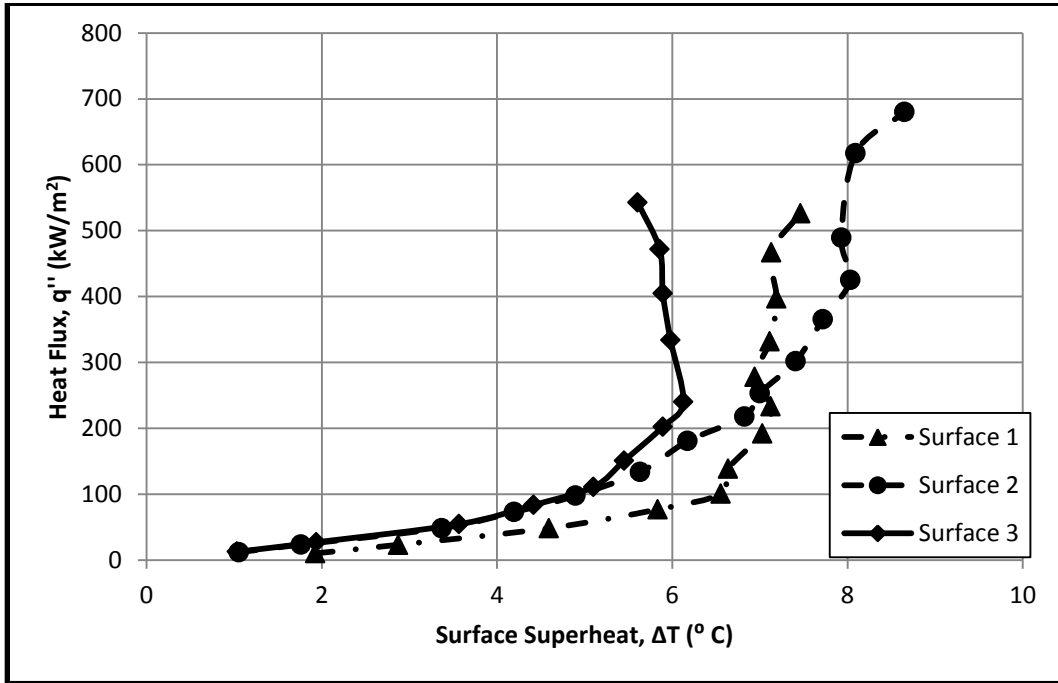


Figure 4.20 Pool boiling curves obtained for boiling nanosuspensions on the three clean surfaces .

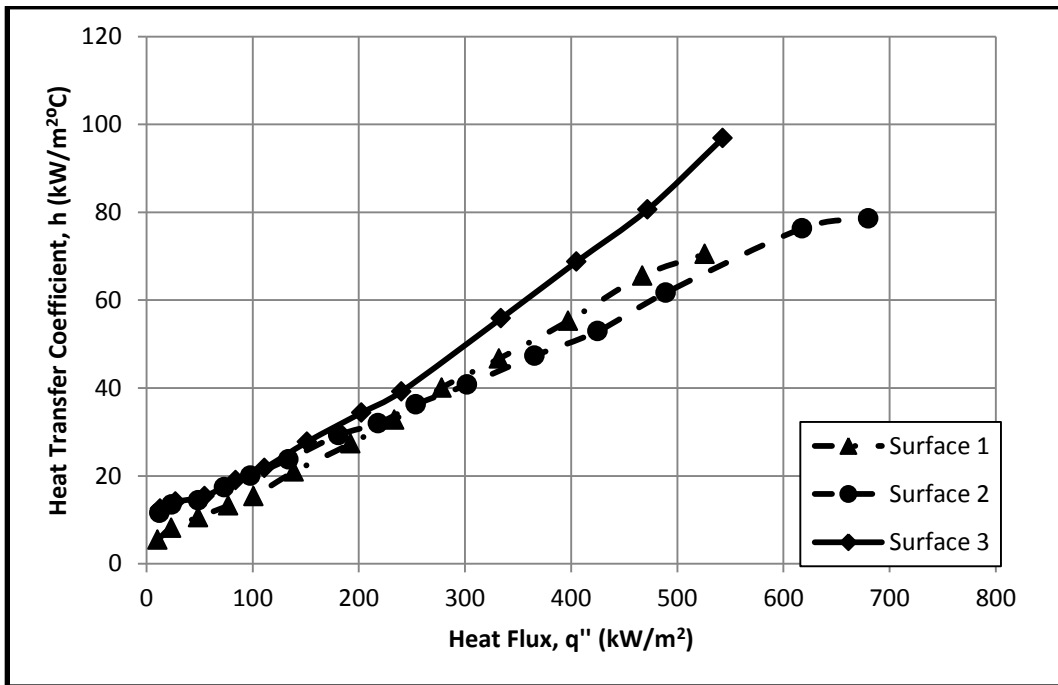


Figure 4.21 Heat transfer coefficient for nanosuspensions on clean surface.

**Table 4.6 Results of surface measurements performed before and after nanosuspensions boiling experiments.**

<i>Surface No.</i>	<i>Preparation method</i>		$R_a$	$R_z$	$PV$	$RMS$	$SIP$
<i>Surface 1</i>	<i>Diamond Turning Machine</i>	<i>Before</i>	5.09	176.91	768.23	12.23	0.5
		<i>After</i>	61.27	1073.53	1688.39	97.38	
<i>Surface 2</i>	<i>Lathe Machine</i>	<i>Before</i>	441.19	5194.09	6020.13	542.29	47.9
		<i>After</i>	473.73	15452.62	18124.50	626.72	
<i>Surface 3</i>	<i>Polishing</i>	<i>Before</i>	464.91	11458.12	13313.55	629.99	46.4
		<i>After</i>	476.06	12031.81	16108.24	628.68	

#### 4.4.5 Distilled Water on Nanosuspensions Deposited Surfaces

In order to investigate the effect of nanoparticles deposition, boiling experiments using distilled water were performed on the nanosuspensions deposited surfaces obtained after the nanosuspensions boiling experiments. The boiling curves of these experiments are shown in Fig.4.22. The corresponding HTC versus the surface heat flux are shown in Fig.4.23.

It can be clearly seen that the maximum HTC occurred in the case of surface 3 (the polished surface), followed by surface 2 and surface 1 (the ultra-smooth surface) .The surface measurements performed before and after these experiments are shown in Table.4.6. The surface measurements for  $R_z$  and  $PV$  show that there is a significant change in the surface texture for all three surfaces. On the other hand, images for the heater surface after boiling nanofluids and nanosuspensions indicate that the presence of the SDBS decreased the nanoparticles deposition as shown in Fig.4.13.

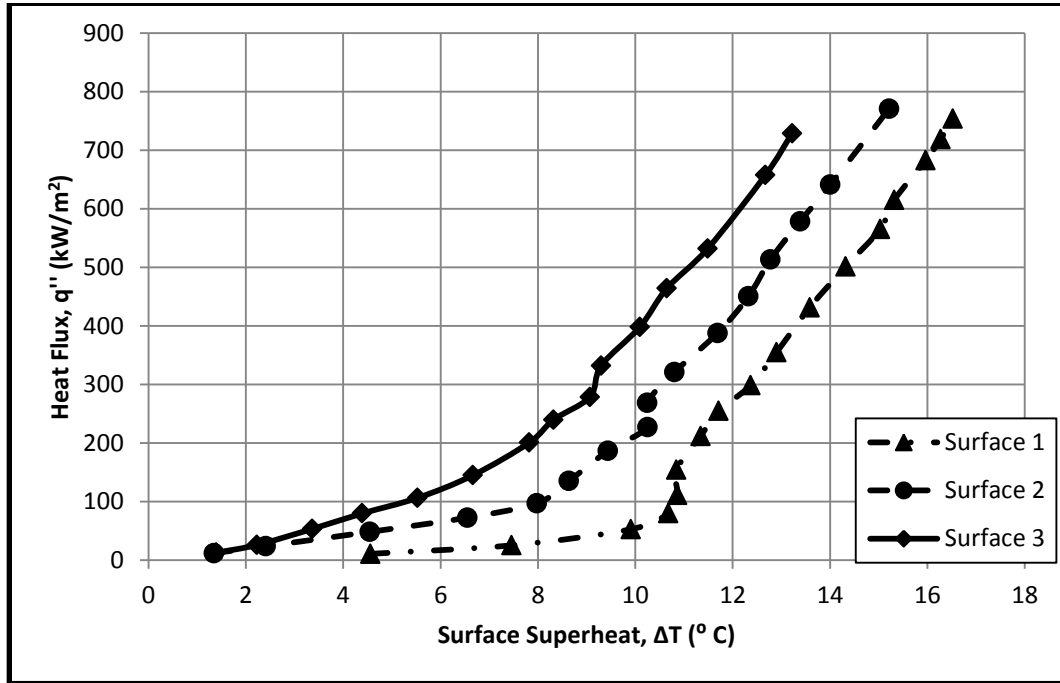


Figure 4.22 Pool boiling curves obtained using distilled water on the three nanosuspensions deposited surfaces (NSDS) .

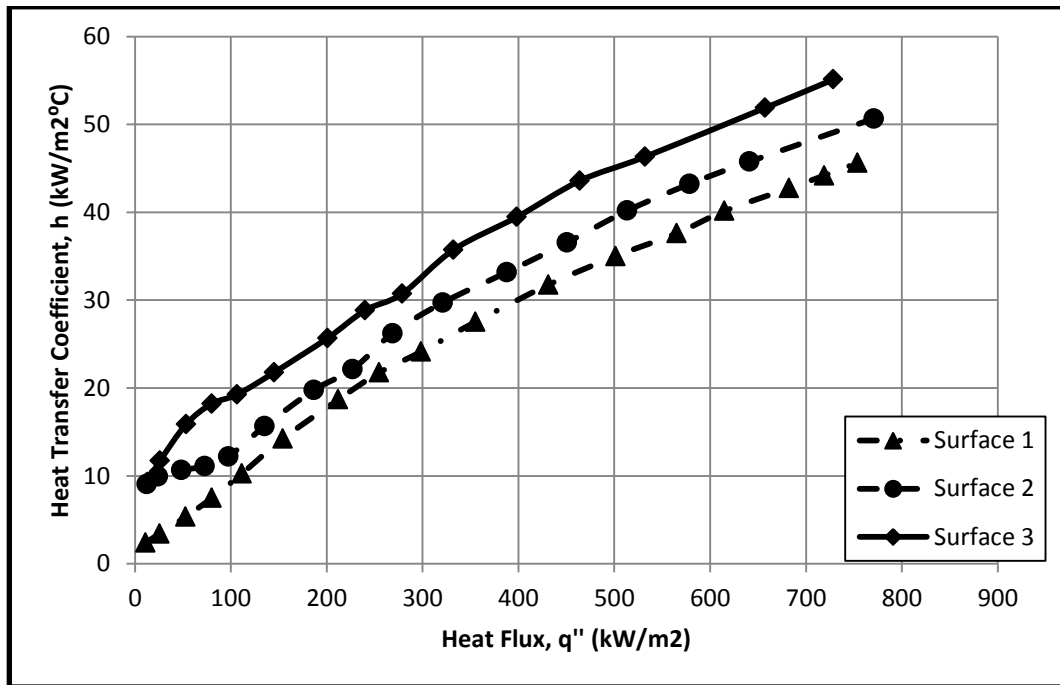


Figure 4.23 Heat transfer coefficient obtained from boiling curves of distilled water on nanosuspensions deposited surfaces (NSDS) .

However, these changes in the surface measurements do not describe the boiling process properly. For example, the surface roughness in the case of nanofluids deposited surface on surface 3 increased from 464.91 nm to 624.08 nm and showed a deterioration with respect to the base fluid on the clean surface, while the surface roughness in the case of nanosuspension deposited surface condition did not change and showed enhancement. This is opposite the what it is reported by many researchers that the rougher surface is, the more heat transfer occurs. These results could be explained as the change in the surface roughness is not reasonable method to quantify the nature nanoparticles porous layer.

#### **4.4.6 SDBS and Distilled Water on Clean Surface**

In order to separate the effect of the SDBS in the nanosuspensions experiments, the SDBS alone was dispersed in distilled water with the same concentration and investigated experimentally. Pool boiling experiments were conducted using the three prepared surfaces. Fig.4.24 shows the boiling curves of the SDBS on the three surfaces. The HTCs versus the corresponding heat fluxes are represented in Fig.4.25. As it is expected, the boiling curve using surface 3 has the highest HTC. Surface 1 and surface 2 have almost the same heat transfer characteristics .

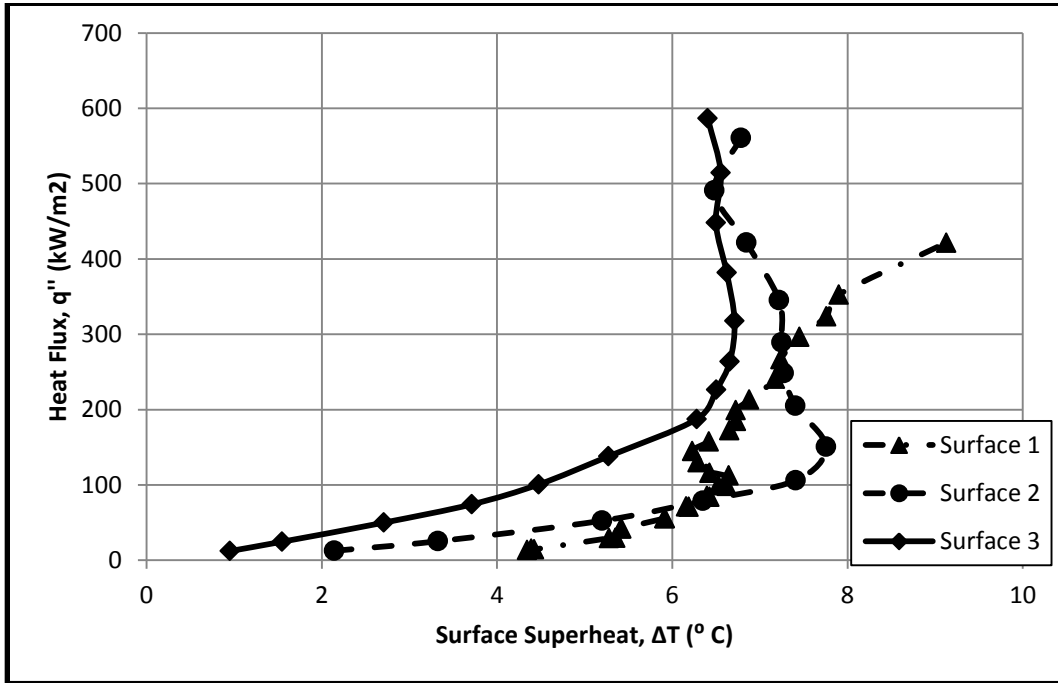


Figure 4.24 Pool boiling curves obtained for boiling SDBS on the three clean surfaces .

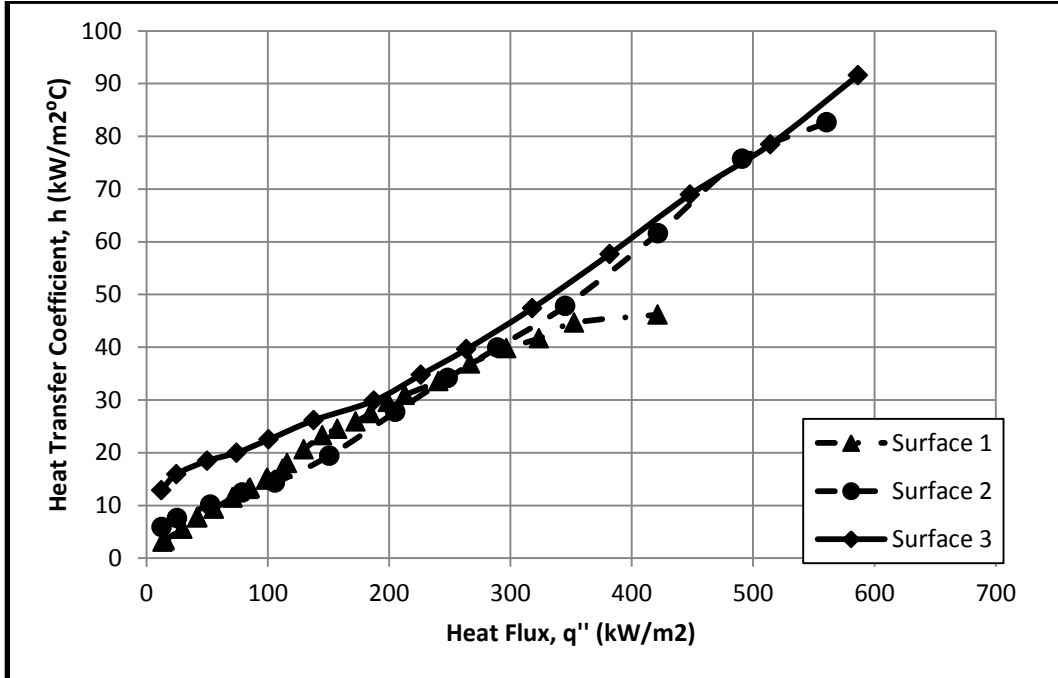


Figure 4.25 Heat transfer coefficient for SDBS on clean surface.

#### 4.4 The Effect of the Transient Nature of the Nanoparticles Deposition Process

The effect of the transient nature of nanoparticles deposition process has been investigated. A test was performed using a constant heat flux of  $313 \text{ kW/m}^2$  (about 25% of the maximum heat input). The constant heat flux was applied for 45 minutes. Changes in the heater surface temperature  $T_s$  were recorded and examined. The test was performed using surface 2 and nanosuspensions. The surface superheat versus time recorded during the test is shown in Fig.4.26. The maximum fluctuation during the test, Fig. 4.26, is less than  $0.9 \text{ }^\circ\text{C}$ . Therefore, the duration time of the experiment is not the main factor that control the nanoparticle deposition rate.

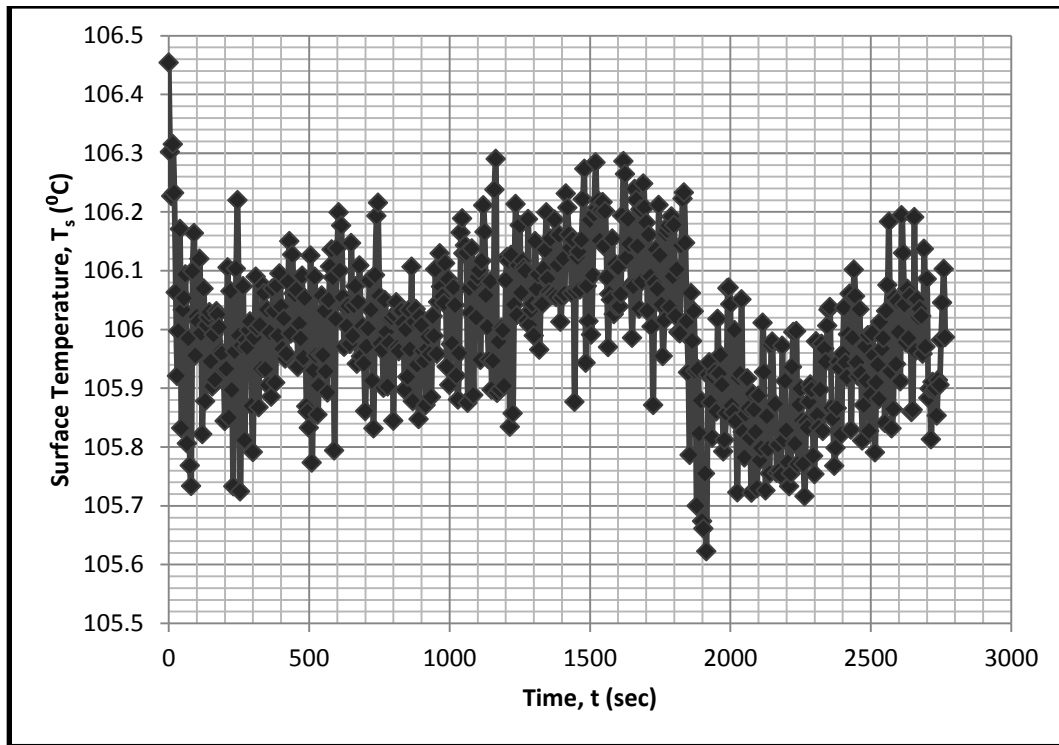


Figure 4.26 Heater Surface fluctuations during the test.

## **Chapter 5 Summary, Conclusion and Recommendations for Future Work**

### **5.1 Summary and Conclusion**

An experimental investigation was carried out to study the effect of surface preparation method on pool boiling of pure water and nanofluids. The boiling surface was prepared using three different methods, namely, machining using a diamond turning machine, machining using a conventional lathe, and polishing using emery sandpaper. The average surface roughness of the first surface was 6 nm and 470 nm for the other two surfaces. The boiling surface used in this study is a flat copper disc with a diameter of 25.4 mm. Nanoparticles with an initial particle diameter of 10 nm and constant concentration of 0.05%wt was used throughout the present study. In order to enhance the nanofluids stability and reduce particles deposition on the heater surface, [27, 28], a surfactant (SDBS) was added to the nanofluids with a concentration of 0.1%wt. In this study, distilled water, nanofluids, distilled water plus SDBS surfactant, and nanofluids mixed with SDBS (nanosuspensions) were boiled on clean surfaces. Distilled water boiling experiments were carried out after the nanofluids and nanosuspensions experiments to assess the change of the surface characteristics due to nanoparticles deposition. The same experiments were conducted on the three prepared surfaces.

The heat transfer coefficient on machined surfaces (the ultra-smooth and rough surfaces) was enhanced in the case of nanofluids and nanosuspensions with respect to the base fluid (pure water). The distilled water boiling experiments on the nanoparticles deposited surface showed that the heat transfer behavior is almost similar to that of distilled water on the clean surfaces, which means that nanoparticles deposition was



minimal and the enhancement in the heat transfer rate was due to the change in the thermo-physical properties of the nanofluids, and not due to the change in the surface texture.

A similar trend was found in the case of surface 3 (polished surface), in such case, the use of nanoparticles enhanced the rate of heat transfer. However, the boiling curves obtained using distilled water boiled on unclean surfaces were shifted to the left compared to the boiling curves of distilled water on the clean surfaces. These results are due to nanoparticles deposition which was more pronounced in the case of surface 3. Images of the boiling surfaces and surface measurements taken before and after the nanofluids and nanosuspensions experiments showed that the heat transfer behaviour depends significantly on boiling surface preparation method.

The use of SDBS surfactant as a dispersing agency has increased the heat transfer dramatically. This could be explained as the surfactant decreases the surface tension which is the main cause of such enhancement.

The measurements of the surfaces roughness before and after the nanofluids experiments have shown that the difference in the measurements is not the proper tool to describe the porous layer that forms on the heater surface. In other words, increase or decrease the surface roughness due to the nanoparticles' deposition does not predict the boiling process on the coated surfaces as it is the case in clean surfaces.

The current results have shown that boiling surfaces prepared by using emery sandpaper tend to have a larger number of active nucleation sites.

## **5.2 Recommendation for Future Work**

Since it is not clear whether the deposited nanoparticles multiply or deactivate the nucleation site, boiling of nanofluids could be better understood by studying bubble dynamics and the interaction of nanoparticles with active nucleation sites. This might be possible by performing boiling experiments on transparent surfaces such as silicon wafer so that the change in the number of nucleation sites can be detected.

## Bibliography

- [1] Frank P. Incropera, David P. DeWitt , Theodore L. Bergman , Adrienne S. Lavine, Fundamentals of Heat and Mass Transfer, John Wiley & Sons, 2006.
- [2] Collier, John G. and Thome, John R., Convective Boiling and Condensation, Oxford: Oxford University Press, 1965.
- [3] S. Nukiyama, "Maximum and minimum values of heat  $q$  transmitted from metal to boiling water under atmospheric pressure," *The Japan Society of Mechanical Engineers Jpn. ,* vol. 37, no. 53-54, pp. 367-374, 1934.
- [4] S. U. S. Choi, " Enhancing Thermal Conductivity of Fluids with Nanoparticles, in Developments and Applications of Non-Newtonian Flows," *American Society of Mechanical Engineers, New York,* vol. FED 231, pp. 99-105, 1995.
- [5] J. C. Maxwell, in *Treatise on Electricity and Magnetism*, Oxford, Clarendon Press, 1873.
- [6] Sarit Kumar Dasa, Stephen U. S. Choib & Hrishikesh E. Patel, "Heat Transfer in Nanofluids—," *Heat Transfer Engineering,* vol. 27, no. 10, pp. 3-19, 2006.
- [7] G. Harish, V. Emlin, V. Sajith, "Effect of surface particle interactions during pool boiling of nanofluids," *International Journal of Thermal Sciences,* vol. 50, no. 12, pp. 2318-2327, 2011.
- [8] A. Abdelhady, "EXPERIEMENTAL INVESTIGATION OF POOL BOILING AND BOILING UNDER SUBMERGED IMPINGING JET OF NANOFLUIDS," McMaster University, Hamilton, Ontario, Canada, 2013.
- [9] G. Prakash Narayan, K. B. Anoop, and Sarit K. Das, "Mechanism of enhancement/deterioration of boiling heat transfer using stable nanoparticle suspensions over vertical tubes," *Journal of Applied Physics,* vol. 102, no. 7, p. 074317, 2007.
- [10] Eastman JA, Choi SUS, Li S, Yu W, Thomson LJ, "Anomalously increased effective thermal conductivities of ethylene glycol-based nanofluids containing copper nanoparticles.," *Applied Physics Letters,* vol. 87, no. 6, pp. 718-720, 2001.

- [11] Michael P. Beck, Yanhui Yuan, Pramod Warriar, Aryn S. Teja, "The thermal conductivity of alumina nanofluids in water, ethylene glycol, and ethylene glycol + water mixtures," *Journal of Nanoparticle Research*, vol. 12, no. 4, pp. 1469-1477, 2010.
- [12] Peter Vassallo a, Ranganathan Kumar , Stephen D'Amico, "Pool boiling heat transfer experiments in silica–water nano-fluids," *International Journal of Heat and Mass Transfer*, vol. 47, no. 2, p. 407–411, 2004.
- [13] I.L. Piro, W. Rohsenow , S.S. Doerffer, "Nucleate pool-boiling heat transfer.I: review of parametric effects of boiling surface," *International Journal of Heat and Mass Transfer*, vol. 47, no. 23, p. 5033–5044, 2004.
- [14] Kang, Myeong-Gie, "Effect of surface roughness on pool boiling heat transfer," *International Journal of Heat and Mass Transfer*, vol. 43, no. 22, p. 4073±4085, 2000.
- [15] Benjamin J. Jones, John P. McHale, Suresh V. Garimella, "The Influence of Surface Roughness on Nucleate Pool Boiling Heat Transfer," *Birck and NCN Publications*, p. 480, 2009.
- [16] Robert A. Taylor, Patrick E. Phelan, "Pool boiling of nanofluids: Comprehensive review of existing data and limited new data," *International Journal of Heat and Mass Transfer*, vol. 52, no. 23-24, p. 5339–5347, 2009.
- [17] Sarit K. Das a, Nandy Putra b, Wilfried Roetzel, "Pool boiling characteristics of nano-fluids," *International Journal of Heat and Mass Transfer*, vol. 46, no. 5, p. 851–862, 2003.
- [18] Chang, Cheol Bang and Soon Heung, "Boiling heat transfer performance and phenomena of Al<sub>2</sub>O<sub>3</sub>–water nano-fluids from a plain surface in a pool," *International Journal of Heat and Mass Transfer*, vol. 48, no. 12, p. 2407–2419, 2005.
- [19] Dongsheng Wen, Michael Corr , Xiao Hua, Guiping Lin, "Boiling heat transfer of nanofluids: The effect of heating surface modification," *International Journal of Thermal Sciences*, vol. 50, no. 4, p. 480–485, 2011.
- [20] S.J. Kim, I.C. Bang , J. Buongiorno , L.W. Hub, "Surface wettability change during pool boiling of nanofluids and its effect on critical heat flux," *International Journal*

*of Heat and Mass Transfer*, vol. 50, no. 19-20, p. 4105–4116, 2007.

- [21] Sang M. Kwark, Ratan Kumar , Gilberto Moreno , Jaisuk Yoo , Seung M. You, "Pool boiling characteristics of low concentration nanofluids," *International Journal of Heat and Mass Transfer*, vol. 53, no. 5-6, p. 972–981, 2010.
- [22] Saeid Vafaeia, Theodorian Borca-Tasciuc, "Role of nanoparticles on nanofluid boiling phenomenon : Nanoparticle deposition," *Chemical Engineering Research and Design*, vol. 92, no. 5, p. 842–856, 2014.
- [23] O. Ahmed, M.S. Hamed, "Experimental investigation of the effect of particle deposition on pool boiling of nanofluids," *International Journal of Heat and Mass Transfer*, vol. 55, no. 13-14, p. 3423–3436, 2012.
- [24] Johnathan S. Coursey, Jungho Kim, "Nanofluid boiling: The effect of surface wettability," *International Journal of Heat and Fluid Flow*, vol. 29, no. 6, p. 1577–1585, 2008.
- [25] O. Ahmed, M.S. Hamed, "Experimental investigation of the effect of particle deposition on pool boiling of nanofluids," *International Journal of Heat and Mass Transfer*, vol. 55, no. 13-14, p. 3423–3436, 2012.
- [26] Holman, J. P., *Experimental Methods for Engineers*, New York: McGraw-Hill, 2001.
- [27] Xian-ju Wang, Xinfang Li, and Shuo Yang, "Influence of pH and SDBS on the Stability and Thermal Conductivity of Nanofluids," *Energy & Fuels*, vol. 23, no. 5, p. 684–2689, 2009.
- [28] T. Yousefi, E. Shojaeizadeh , H.R. Mirbagheri , B. Farahbaksh , M.Z. Saghir, "An experimental investigation on the impingement of a planar jet of Al<sub>2</sub>O<sub>3</sub>–water nanofluid on a V-shaped plate," *Experimental Thermal and Fluid Science*, vol. 50, p. 114–126, 2013.
- [29] W. Frost, C.J. Kippenhan,, "Bubble growth and heat transfer mechanisms in the forced convection boiling of water containing a surface active agent," *International Journal of Heat and Mass Transfer* , vol. 10, no. 7, p. 931–949, 1967.
- [30] Wu-Tsann Wut, Chic-Lun Hu, Yu-Min Yang, "Surfactant Effect on Boiling Incipience and Bubble Growth Dynamics of. Surface Boiling in Water," *journal of chinese institute of chemical engineer*, vol. 24, p. 111–118, 1993.

- [31] Piroo, I.L., "Experimental evaluation of constants for the Rohsenow pool boiling correlation," *International Journal of Heat and Mass Transfer*, vol. 42, no. 11, pp. 2003-2013, 1999.
- [32] Rohsenow, B. B. Mikic and W. M., "A New Correlation of Pool-Boiling Data Including the Effect of Heating Surface Characteristics," *Journal of Heat Transfer*, vol. 91, no. 2, pp. 245-250, May 01, 1969.
- [33] S. J. Kim, I. C. Bang, J. Buongiorno, and L. W. Hu, "Effects of nanoparticle deposition on surface wettability influencing boiling heat transfer in nanofluids," *Applied Physics Letters*, vol. 89, no. 15, p. 153107, 2006.